

Development and Validation of a Multi-Material
Extrusion Additive Manufacturing Method

by

Ryan L. Hemphill

A thesis submitted to the Faculty and the Board of Trustees of the Colorado School of Mines in partial fulfillment of the requirements for the degree of Master of Science (Mechanical Engineering).

Golden, Colorado

Date _____

Signed: _____
Ryan L. Hemphill

Signed: _____
Dr. Douglas L. Van Bossuyt
Thesis Advisor

Golden, Colorado

Date _____

Signed: _____
Dr. Gregory Jackson
Professor and Head
Department of Mechanical Engineering

ABSTRACT

The adoption of Additive Manufacturing (AM) for low production run parts has created the need for more versatile AM materials to aid engineers, students, enthusiasts, and the maker community. Current low cost AM processes (e.g.: material extrusion and vat photopolymerization) have limited materials that are questionably suitable for load bearing components. A composite approach to AM can improve mechanical properties of components by integrating multiple developed materials, thus gathering the beneficial material properties of each separate material in an AM-produced composite. In this thesis, I present the development and validation of two composite AM processes through multiple material testing case studies. Throughout the validation procedure, I explore variations in matrix material, infill density, infill type, and fiber reinforcement. 2D localized strain analysis is presented via digital image correlation to analyze coupon failures, multi-material interactions, and infill and fiber-reinforcement effectiveness. Material testing shows distinct differences in samples produced from the same two or three materials and demonstrates how mechanical property improvement can be achieved through design for tunable materials given a geometric constraint. Implementation of this process is a step towards achieving tunable material properties for low cost AM technologies.

TABLE OF CONTENTS

ABSTRACT.....	iii
LIST OF FIGURES	viii
LIST OF TABLES.....	ix
LIST OF ABBREVIATIONS.....	x
ACKNOWLEDGMENTS	xii
CONTRIBUTION OF OTHERS.....	xiii
CHAPTER 1 INTRODUCTION	1
1.1 Intellectual Merit.....	1
1.2 Broader Impacts	2
1.3 Thesis Organization	2
CHAPTER 2 LITERATURE REVIEW	4
2.1 AM Toolchain.....	4
2.2 Material Extrusion	4
2.2.1 Fused Filament Fabrication (FFF)	5
2.3 Vat Photopolymerization	6
2.3.1 SLA.....	7
2.3.2 DLP SLA	8
2.3.3 Photopolymers	9
2.4 Binder Jetting	10
2.5 Material Jetting	11
2.6 Powder Bed Fusion.....	11
2.7 Directed Energy Deposition.....	11
2.8 Sheet Lamination	12
2.9 Composites.....	12

2.9.1	Short Fiber Reinforcement.....	13
2.9.2	Long Fiber Reinforcement.....	13
2.9.3	Global Fiber Reinforcement	13
2.9.4	FRP Failures.....	14
2.10	Composite AM Technologies	14
2.10.1	Reinforced Filaments	15
2.10.2	Doped Filaments	15
2.10.3	Ultrasonic/Thermal Embedding.....	16
2.10.4	Multifunctional and Tunable Materials	16
2.11	2D DIC Strain Analysis	16
CHAPTER 3 MANUFACTURING COMPOSITES USING A HYBRID MATERIAL EXTRUSION-PHOTOPOLYMERIZATION METHOD.....		17
3.1	Introduction.....	17
3.2	Background.....	20
3.2.1	AM Toolchain.....	20
3.2.2	Fused Filament Fabrication.....	21
3.2.3	Stereolithography (SLA).....	22
3.2.4	AM Materials	22
3.2.5	Composites.....	23
3.2.6	Composite AM Technologies	23
3.3	Development and Validation of F3SLA	24
3.3.1	F3SLA Development	24
3.3.2	F3SLA Validation.....	28
3.4	Experimental Results	32
3.4.1	Tensile Data	32
3.4.2	Compressive Data	34

3.4.3	Summary	35
3.5	Discussion	37
3.6	Future Work	39
3.7	Conclusion	40
CHAPTER 4	DEVELOPMENT AND VALIDATION OF AN ECONOMICAL POLYMER FIBER-REINFORCED COMPOSITE ADDITIVE	41
4.1	Introduction.....	42
4.2	Background	44
4.2.1	Material Extrusion	44
4.2.2	Vat Photopolymerization	46
4.2.3	AM Toolchain.....	48
4.2.4	Composites.....	48
4.2.5	Composite AM Technologies	50
4.2.6	Multifunctional and Tunable Materials	52
4.3	Development of RF3SLA	53
4.4	Material Testing of RF3SLA Parts	55
4.4.1	Coupon Production	56
4.4.2	Material Testing	56
4.5	Results.....	58
4.5.1	Photopolymer RF3SLA	58
4.5.2	Epoxy RF3SLA.....	59
4.5.3	Result Summary.....	60
4.6	Discussion	62
4.7	Conclusion and Future Work	65
CHAPTER 5	AUTOMATION	67
5.1	Steps Already Taken	67

5.2	Process Issues and Future Work	71
CHAPTER 6	CONCLUSIONS.....	72
6.1	Research Contributions	72
6.1.1	F3SLA Case Study Conclusions.....	72
6.1.2	RF3SLA Case Study Conclusions	73
6.2	Broader Impact.....	73
6.3	Future Work	74
6.4	Closing Thoughts	75
REFERENCES CITED.....		77
APPENDIX A.....		88
APPENDIX B.....		90

LIST OF FIGURES

Figure 2.1: Fused Filament Fabrication Extrusion	6
Figure 2.2: Typical “Top Down” SLA Configuration	8
Figure 2.3: Typical “Bottom Up” DLP Configuration	9
Figure 3.1: Possible F3SLA Gantry Setup.....	26
Figure 3.2: Manual Photopolymer Deposition Process	27
Figure 3.3: F3SLA Adhesion Tests	27
Figure 3.4: F3SLA Samples.....	28
Figure 3.5: Sample 2D DIC Strain Field Overlay (100% DLP).....	30
Figure 3.6: Tensile Coupon Geometry (mm).....	32
Figure 3.7: Control Stress-Strain Curves	33
Figure 3.8: F3SLA Stress-Strain Curves	33
Figure 3.9: Control Compressive (-) Stress-Strain Curves	34
Figure 3.10: F3SLA Compressive (-) Stress-Strain Curves.....	35
Figure 4.1: Possible RF3SLA Extruder Carriage Setup	54
Figure 4.2: RF3SLA Sample.....	55
Figure 4.3: Sample 2D DIC Strain Field Overlay (100% Infill FFF).....	57
Figure 4.4: RF3SLA Stress-Strain Curves (Photopolymer)	59
Figure 4.5: RF3SLA Stress-Strain Curves (Epoxy).....	60
Figure 5.1: RF3SLA Process Diagram	68
Figure 5.2: Envisioned RF3SLA Extruder Setup	69
Figure 5.3: Current Extruder Setup.....	70
Figure 5.4: RF3SLA Printer in UV Safety Enclosure.....	70

LIST OF TABLES

Table 3.1: F3SLA Case Study Overview.....	31
Table 3.2: F3SLA Case Study Results Summary	35
Table 3.3: Process Recommendation for Various Parameters.....	39
Table 4.1: RF3SLA Case Study Overview	55
Table 4.2: RF3SLA Case Study Results Summary	62
Table 4.3: RF3SLA Recommendations	65

LIST OF ABBREVIATIONS

Acrylonitrile Butadiene Styrene	ABS
American Society for Testing and Materials	ASTM
Computer Aided Design	CAD
Continuous Fiber Reinforced Polymers.....	CFRP
Continuous Fiber Reinforced Thermoplastics	CFRT
Digital Image Correlation	DIC
Directed Light Fabrication.....	DLF
Direct Metal Deposition.....	DMD
Direct Write	DW
Electron Beam Melting.....	EBM
Finite Element Analysis	FEA
Global Fiber Reinforced Polymers	GFRP
High Impact Polystyrene.....	HIPS
Initial Graphics Exchange Specification.....	IGES
Laser Engineered Net Shaping.....	LENS
Long Fiber Reinforced Polymers.....	LFRP
Long Fiber Reinforced Thermoplastic.....	LFRT
Laminated Object Manufacturing	LOM
Resin Injection Molding	RIM
Resin Transfer Molding	RTM
Short Fiber Reinforced Polymers.....	SFRP
Short Fiber Reinforced Thermoplastic.....	SFRT
Selective Laser Melting	SLM
Selective Laser Sintering	SLA

Subtractive Manufacturing.....	SM
Ultrasonic Additive Manufacturing	UAM
Ultra-Violet	UV
Vat Photopolymerization	VP
Digital Light Processing	DLP
Fused Filament Fabrication.....	FFF
Fiber Reinforced Polymers	FRP
Stereolithography	SLA

ACKNOWLEDGMENTS

This research would not have been possible without the support of many different people on many different levels. I would first like to recognize the support of Douglas Van Bossuyt, my research advisor, who provided research insight, coursework, mentoring, funding, and a genuine interest in this research. I would also like to recognize Aaron Stebner and the Colorado School of Mines Beam Team including Garrison Hommer and Andy Peterson who provided testing equipment and technical assistance. Additionally, I would like to acknowledge the efforts of Kevyn Young, Maxwell Harris, and Adam Short who aided in the initial development and testing of F3SLA. Finally, I would like to thank my family and all the friends I have made throughout my educational career for their continued support.

CONTRIBUTION OF OTHERS

Douglas Van Bossuyt provided editing assistance, research advice, and funding throughout this thesis. Aaron Stebner provided material testing equipment and research advice on the case studies presented in Chapters 3 and 4. Kevyn Young, Maxwell Harris, and Adam Short provided research assistance on preliminary idea conceptualization and initial testing. Kyle Kneable provided coupon preparation assistance and hardware manufacturing assistance. Garrison Hommer provided research advice on experimental design and speckling of test coupons. Andy Peterson provided code for load frame operation and image acquisition.

CHAPTER 1 INTRODUCTION

A need for a low cost polymer Additive Manufacturing (AM) process that is capable of producing load-bearing components with a wide range of achievable properties has recently arisen. While economical AM has helped to streamline the design process and provided a rapid and relatively inexpensive option for prototyping, the use of AM for end use parts is still in its infancy [1]. Several major factors have led to the premature adoption of low-end polymer AM for end-use components including: 1) the widespread availability of low cost AM machines including material extrusion and vat photopolymerization, online businesses focused on economical quick turnaround manufacturing of AM parts, and community funding of projects [2–4]. This thesis proposes an economical composite AM approach through two processes to achieve improved mechanical integrity and material tunability for low cost polymer AM. The layer-based manufacturing approach seen in many AM processes is uniquely suitable for composite materials and tunable material parameters due to discrete deposition or curing/sintering of feedstock material. This thesis presents process validation through material testing data demonstrating how material properties can be tuned to achieve desired part performance.

1.1 Intellectual Merit

This thesis presents the framework and validation of two economical polymer composite AM processes that allow more design freedom and flexibility to students, engineers, enthusiasts, and the maker community. These composite AM processes integrate thermoplastics, photopolymers, epoxies, thermosets, and additional materials such as fiber-reinforcement to achieve a desired set of material properties. The process approach specifically focuses on the direct manufacture of multi-material AM components from digital design. Through the implementation of these

composite AM processes, economical load-bearing components can be manufactured with mechanical integrity.

1.2 Broader Impacts

Public interest in AM has greatly increased in the last decade due in part to the promise of manufacturing parts at home with the click of a button. Printing products at home interests the public because it brings rapid access to products to a whole new level, theoretically allowing online shoppers to receive purchased goods almost instantaneously and without having to leave the home [5]. The technical community including engineers, scientists, manufacturers, and hobbyists see AM as a design tool, prototyping tool, and low production run manufacturing tool [6]. Mass customization of parts and products is a key benefit of AM for both the public and the technical community due to AM's unique suitability for low production runs. Personalized goods such as unique colors, patterns, engravings, textures, and geometries are limited in mass production by factors such as the number of production lines constructed and tooling costs [7]. AM overcomes traditional mass production customization limitations by allowing the manufacture of a wide range of parts and products on a single production line without retooling costs[8]. The hobbyist and maker community can immediately benefit from the composite AM processes developed in this thesis by implementing the processes on hobbyist AM machines. I expect the composite AM processes to become available to engineers and AM service houses in the near future as commercial machines are developed to implement the processes developed in this thesis. To that end, two provisional patents have already been filed on the work presented here.

1.3 Thesis Organization

This thesis is organized into six chapters including two journal articles prepared for submission. Chapter 2 provides a literature review on several relevant areas including current AM technologies, current composite AM technologies, composites, AM materials, and optical strain analysis for

validation of samples. Chapter 3 presents the first composite AM process and a material testing validation case study through written material prepared for journal submission. Chapter 4 present the second composite AM process also prepared for journal submission and a material testing validation case study. Chapter 5 presents an automation scheme, steps taken to date, and future work. The thesis concludes in Chapter 6 with a review of key contributions.

CHAPTER 2 LITERATURE REVIEW

The seven categories of Additive Manufacturing (AM) as defined by the ASTM F42 – Additive Manufacturing Committee are Material Extrusion, Vat Photopolymerization, Binder Jetting, Material Jetting, Powder Bed Fusion, Directed Energy Deposition, and Sheet Lamination [9]. Of these, the economically priced and commercially available options for startups, hobbyists, and enthusiasts are Material Extrusion and Vat Photopolymerization machines. While costs are steadily decreasing for several other polymer technologies including Binder Jetting and Material Jetting, there are currently no commercial machines marketed towards the low cost sector.

2.1 AM Toolchain

The polymer AM toolchain begins with the modeling of a 3D part in a CAD environment. Once modeled, this CAD file is exported as a file that can be interpreted by slicer software. The most commonly used file type is the stereolithography (STL) format although other options do exist (IGES, AMF, etc.) [10–12]. STL files have been suitable for AM machines up until the incorporation of multiple materials and colors where more information is needed. Many different file types that enable more information to be stored (material, color, etc.) are currently under development and testing [13]. Once converted, the mesh file is then loaded into a slicer. The slicer generates 2D cross sectional slices of the 3D part and then generates a toolpath in order to fill each cross section via a layer based approach [12]. This toolpath is then exported as g-code and uploaded to the machine controller. The controller can then execute the toolpath completing the 3D part.

2.2 Material Extrusion

Material extrusion is the most common AM method in use today due to its widespread adoption in desktop 3D printers [14]. The basic principle behind material extrusion is the

deposition of a material through a nozzle at discrete locations in a build volume [15]. In order for this principle to work, material extrusion machines require three axes of motion, a material that can flow through a nozzle, and control over the flow of material [15]. Material extrusion typically requires four actuators for a single extruder setup to achieve three axes of motion plus one axis of extrusion. Material extrusion's popularity comes from the low barrier to entry, ease of use, relatively simplistic controls, and stable, safe feedstock materials.

2.2.1 Fused Filament Fabrication (FFF)

Fused Filament Fabrication (FFF), or Fused Deposition Modeling¹ (FDM) [15], is a common material extrusion method primarily found in inexpensive hobbyist and prototyping AM. This method extrudes polymer filaments through a hot end as shown in Figure 2.1. The hot end heats a plastic filament past the filaments glass transition temperature allowing the filament to flow through the nozzle when advanced by an actuator. The extruder assembly is mounted on a three axis gantry to lay down material according to a predefined toolpath. The toolpath is generated by a slicer program that imports 3D CAD geometry, slices the object into 2D cross sections, determines a path to fill each cross section based on user preferences, and exports the toolpath in the form of g-code. The FFF process is described in greater detail in [16].

FFF machines typically use thermoplastics as feedstock for creating parts due to the relatively low glass transition temperature of thermoplastics and mechanical characteristics including strength and ductility [17]. Thermoplastics are commonly used in other manufacturing processes such as injection molding and vacuum forming [18,19]. However, parts manufactured via FFF exhibit anisotropic mechanical properties [20]. Due to the anisotropic nature of FFF parts, real-world mechanical properties usually fall well below bulk material properties [21].

¹ Registered trademark of Stratasys, Inc., Eden Prairie, MN; www.stratasys.com

Thermoplastics also exhibit mechanical property degradation at every recycling phase [22]. This both limits the reuse of feedstock and adds a layer of complexity to predicting thermoplastic mechanical properties in design.

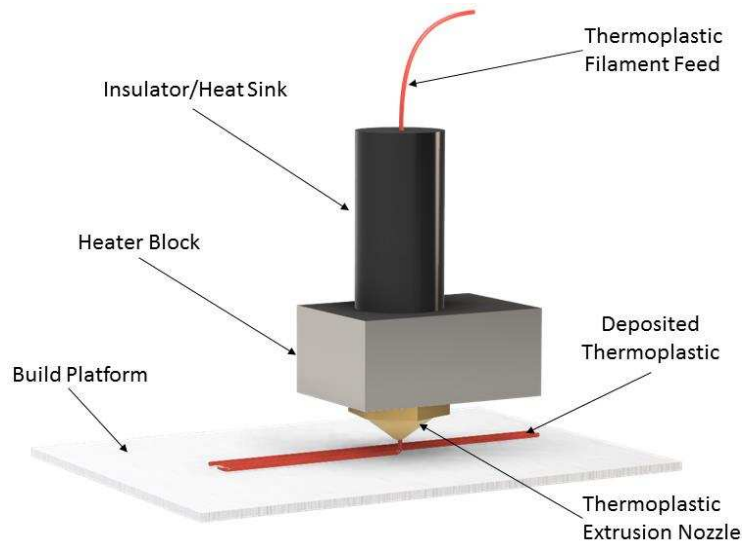


Figure 2.1: Fused Filament Fabrication Extrusion

2.3 Vat Photopolymerization

Vat Photopolymerization (VP) refers to a group of AM technologies that utilize photopolymers and a light source to cure successive layers resulting in full 3D parts. The two commonly used AM technologies in this category are Stereolithography (SLA) and a modified SLA technique using Direct Light Processing² (DLP) [23,24]. Photopolymers are cured via a process called photo polymerization usually initiated by ultra violet (UV) light in both of the SLA and DLP methods [16,25]. The core SLA process was first developed in the 1960's and therefore is a more mature process than many AM processes [16].

There are two common machine setups for VP including “top down” and “bottom up” [24]. Top down AM configurations consist of an actuated build platform with a full tank of material

² Registered trademark of Texas Instruments, Inc., Dallas, TX; www.ti.com

while bottom up AM configuration add material one layer at a time. For VP, bottom up configurations typically consist of a smaller vat of material, as opposed to top down, and an actuated build platform that moves away from the vat [26]. Top down is the traditional method for VP that uses a large photopolymer tank and a platform that is lowered into the tank. In this setup, the bottom layer of the part is cured first while the build platform is then lowered for each successive layer to be cured to the previous layer. Bottom up configurations, while taking an opposite approach by moving the build platform away from the resin tank at each new layer, also build from the bottom layer to the top layer. Bottom up can use a much shallower photopolymer tank as only a layer height of photopolymer theoretically needs to be in the tank for each layer. VP processes typically achieve the best accuracy and surface finish across all AM techniques [16]

2.3.1 SLA

SLA VP uses photopolymers to successively build up layers into a finished 3D part. This method uses a laser beam to cure the photopolymer. A fixed laser is aimed at a scanning galvanometer that focuses the laser at discrete locations on the build platform. If there is liquid photopolymer between the beam and the build plate, it is cured by the laser. Tracing the cross section of the part at each layer cures the photopolymer into the correct cross sectional pattern creating a cured layer. SLA VP uses a scanning galvanometer which is an electromechanical actuator that can quickly manipulate a mirror to focus the laser in the desired position determined by the g-code. Some systems incorporate two lasers and optical setups in order to effectively halve the build time although this requires more advanced controls.

SLA is a 1D channel AM technology meaning that it only cures across a line when scanning. Although multiple channels can be added to speed up the build speed, there are several issues that occur between cured photopolymer stand boundaries including shrinkage, curling, and residual stresses [16]. A typical top down SLA configuration is shown in Figure 2.2.

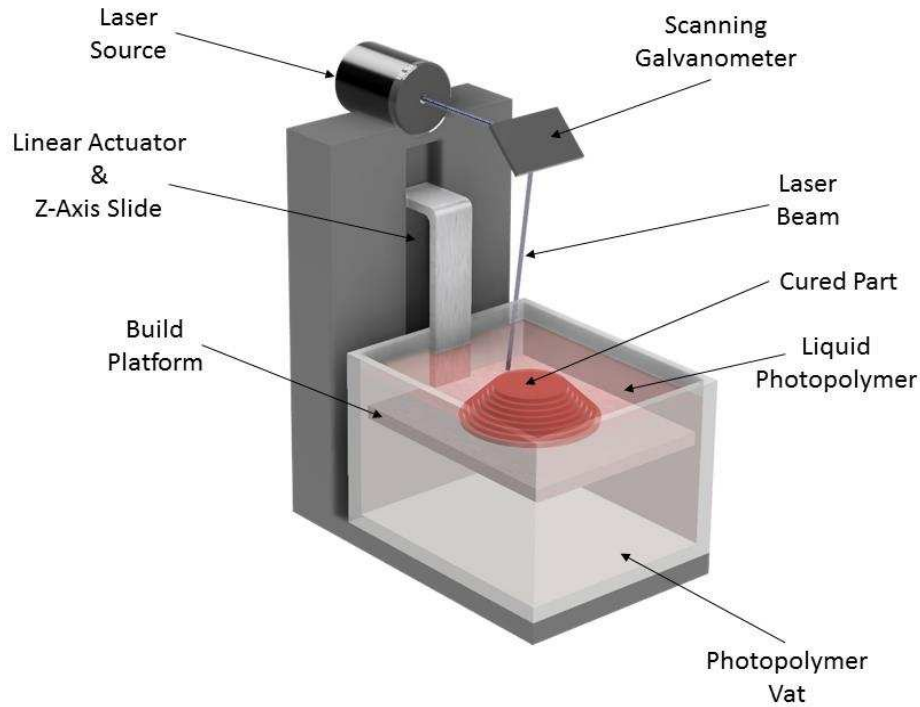


Figure 2.2: Typical “Top Down” SLA Configuration

2.3.2 DLP SLA

DLP additive manufacturing uses a 2D channel approach that cures an entire layer at the same time. This is achieved by using a DLP chip found in most modern digital projectors [16]. The process works by flashing cross sectional patterns of each successive layer at the build plate. Before each image is projected, the build plate is advanced allowing the next layer to build directly on the previous. The benefits of the DLP SLA system are reduction in build time, simple mechanicals and software, and high resolution for small parts [27]. Drawbacks are mainly material related, as with all vat photopolymerization technologies.

Resolution of the DLP chip is directly related to part resolution in DLP SLA. It is easy to create a linear actuator with finer steps to achieve better z resolution by gearing but increasing x-y resolution is more challenging. DLP projectors have a specific resolution due to the number of micro mirrors included. A higher resolution chip results in a higher x-y resolution part. Therefore,

for small parts a full high definition DLP chip can provide significantly better feature resolution than SLS [27]. A typical bottom up configuration DLP system is shown in Figure 2.3.

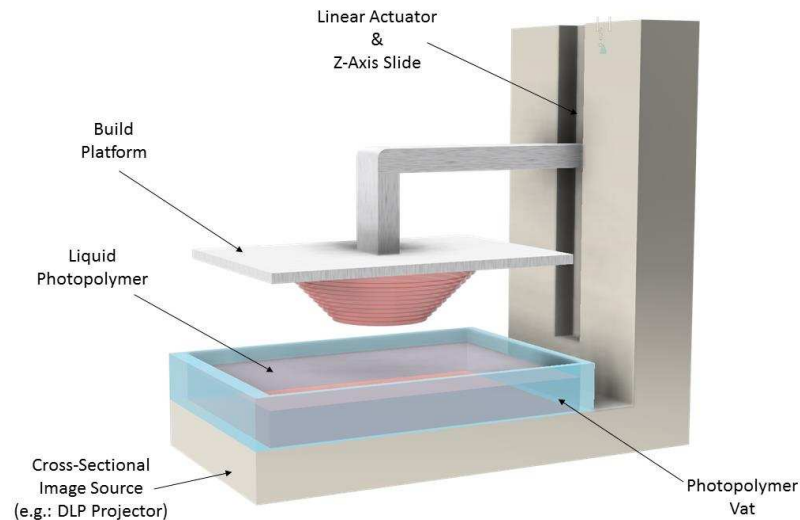


Figure 2.3: Typical “Bottom Up” DLP Configuration

2.3.3 Photopolymers

One issue with photopolymers is the shrinkage that occurs during curing [28]. This shrinkage arises from monomers taking up more volume than their cured polymer counterparts [16]. Curling of individual layers builds stress in a part and can lead to inaccurate part geometry. In order to mitigate curling, a larger build plate bonding force can be used. We have found this can be achieved in multiple ways such as a rougher surface finish or cure time adjustment.

Mechanical properties of photopolymers are less than desirable and can be volatile. This is due to several issues such as UV stability; brittleness; interlayer bonding failure due to uncured photopolymer; warping; and imperfections due to curing reactions such as air pockets, internal thermal stresses, and humidity [29]. Furthermore, mechanical properties of photopolymers directly depend on the mixture of monomers, photoinitiators, diluents, flexibilizers, and stabilizers [16]. Even if each specific blend of photopolymer is tested and cataloged, I have observed that variations in cure times or intensities can still result in inconsistent mechanical properties.

When photopolymers are bombarded by light waves with a specific wavelength dependent on the photoinitiator, typically UV, polymerization occurs [30]. This chemical process cross links monomer chains into larger polymer molecules [30]. Cross linked polymers differ from linear and branched polymer chains, such as those that make up thermoplastics, because they cannot be remelted and recycled [31].

While convenient to use, photopolymers have a whole suite of issues as mentioned before including UV stability, brittleness, interlayer bonding failure due to uncured photopolymer, warping, and imperfections due to curing reactions such as air pockets, internal thermal stresses, and humidity. Photopolymers also cannot be recycled like thermoplastics, and require much more parameter tuning to achieve desired properties than most other materials.

2.4 Binder Jetting

Binder jetting refers to the group of AM technologies that use a powder bed and inkjet printhead for layer based manufacturing [32]. This multi material AM process works by spreading a layer of powder and tracing the cross section of a part with a binder liquid in order to hold the powder together [33]. The process is repeated and layers are stacked until the finished part is constructed. Binder jetting usually requires additional post processing in order to achieve a solid part due to the binder material. The porous part taken directly from the binder jetting machine is called a green part, or green specimen, and is post processed by heat treatments or infiltration of an additional material to achieve desired mechanical properties [16,34,35]. Commonly used infiltrates in binder jetting processes are wax, varnish, lacquer, cyanoacrylate, polyurethane, and epoxies [36]. Binder jetting is one of the few AM technologies that can be used with polymer, metal, and ceramic materials [32].

2.5 Material Jetting

Material jetting is similar to binder jetting although instead of only dispersing a binding agent on a powder bed, material jetting disperses the build material directly [37]. Material jetting works by dispersing build material via a print head directly on a build plate as droplets that are then cured or solidified thermally or by UV light [16]. Once an entire layer is deposited, the next layer is dispersed, gradually building the part layer by layer. Material jetting has been explored using polymers, ceramics, and metals with at least some success in all three categories [38–40].

2.6 Powder Bed Fusion

Powder bed fusion is a group of AM technologies that use a powder bed of bulk material and either a laser or electron beam to sinter or fuse the powder together [41]. The common technologies that fall within this category are Selective Laser Sintering (SLS), Selective Laser Melting (SLM), Electron Beam Melting (EBM), and Direct Metal Laser Sintering (DMLS) [42–45]. A typical powder bed fusion process works by depositing a layer of powder and tracing the cross section of the part on the powder, sintering or melting the powder together [16]. The process is repeated as new layers of powder are deposited and the part is finished. Many different polymer and metals are used in powder bed fusion technologies including Nylon, Stainless Steel, Titanium, and Aluminum [41].

2.7 Directed Energy Deposition

Directed energy deposition processes deposit metals via a wire or powder feed directly onto a build platform [46]. The feedstock material is melted by a focused laser or electron beam during feed in order for bonding to occur [47]. Technologies within the directed energy deposition category include Laser Engineered Net Shaping (LENS), Directed Light Fabrication (DLF), Direct Metal Deposition (DMD), and Laser Direct Casting [16,48]. Directed energy deposition can

theoretically be used for polymer ceramics and metals but in practice is mainly used for metals [16].

2.8 Sheet Lamination

Sheet lamination uses sheets of materials as layers that are bonded via adhesives or welding and cut to each specific cross section [49]. Laminated Object Manufacturing (LOM) and Ultrasonic Additive Manufacturing (UAM) both are included in the sheet lamination category [50–52]. Sheet lamination technologies integrate both additive and subtractive manufacturing processes because despite using a layer based manufacturing approach, the processes requires subtractive manufacturing techniques to trim the sheets into cross sections.

2.9 Composites

Composites use multiple materials in order to achieve a desired set of properties including strength, strain, chemical resistance, strength/weight ratio, etc. Composites are made up of a continuous matrix material and various embedded reinforcement materials, or dispersed phases (e.g.: Glass, Carbon, Kevlar, Metallic, etc.) [53]. Fiber Reinforced Polymers (FRP) are one subset of composites that use various polymers as a matrix [54]. FRPs originally were constructed from polymeric resins reinforced with glass fibers to achieve high strength, stiffness, and chemical resistance while maintaining low cost and weight [54]. Today there are many different FRP combinations including thermoplastics, thermosets, and photopolymers for matrix materials and glass, Kevlar, carbon fiber, etc. for reinforcement [55]. The combination can be customized for each individual application.

Traditional composite manufacturing processes can result in bulk material properties that are near isotropic due to a near random distribution of material units on a molecular scale [56]. Fibers have uniaxial aligned molecular units giving them uniaxial mechanical properties [56]. Composites take advantage of this high strength in one direction by orienting fibers in the direction

of loading. Fiber reinforcement comes in three main categories including short fibers, long fibers, and global fibers [55].

2.9.1 Short Fiber Reinforcement

Short Fiber Reinforced Polymers (SFRP) use a distribution of short reinforcement fibers embedded in the matrix to provide localized reinforcement. SFRP material properties depend on two main parameters including the fiber length distribution and the fiber orientation distribution [57]. Short fiber reinforcement is often used in injection molding and many different methods for determining and/or predicting fiber orientation exist including models and experimental approaches [58,59]. Typically SFRP materials exhibit anisotropic material properties due to a majority of fibers aligning along the flow direction of the matrix material [60]. The critical fiber length is the length of fiber needed to obtain an effective mechanical property benefit (e.g.: higher strength, lower strain) [61]. This factor has been shown to increase with matrix temperature [62].

2.9.2 Long Fiber Reinforcement

Long Fiber Reinforced Polymers (LFRP) are similar to SFRPs with one key difference; longer fibers. Fiber lengths of 6.35 mm (0.25 inch) or greater typically push composites into the LFRP category although this distinction is somewhat arbitrary [63]. LFRP composites have gained popularity in many industries (e.g.: aerospace, automotive) because of their distinct mechanical properties (primarily strength/weight ratio) and ability to be processed in existing manufacturing process (e.g.: injection molding) [64]. Fiber length is not the sole parameter to optimize when designing a composite as it is also important to look at orientation, shear strength of the matrix, surface finish of the fibers [64].

2.9.3 Global Fiber Reinforcement

Global Fiber Reinforced Polymers, also known as Continuous Fiber Reinforced Polymers (CFRP), use identical matrix and phase materials to SFRP and LFRP but use longer fibers [65].

Just as the distinction between Short Fiber Reinforced Thermoplastic (SFRT) and long fiber reinforced thermoplastic (LFRT) composites, the distinction between LFRT and Continuous Fiber Reinforced Thermoplastics (CFRT) is not clearly defined. CFRP composites are desired due to material properties (e.g.: high strength, high impact resistance, Etc.) although they are more difficult to manufacture than SFRT and LFRTs [65].

2.9.4 FRP Failures

FRP composite failures are classified into two different cases including matrix failure and fiber failure [66]. The simplest approach at predicting composite failures is to assume the matrix can support the fibers past their yield strength, therefore only taking into account the strength of the fibers when predicting tensile failure [67]. This is not physically the case in many instances and therefore better models that look at both matrix fiber bonding forces and fiber strength as separate failure cases have been developed [66].

A composite matrix transfers the load to reinforcement fibers via shear stress [56]. Additionally, the matrix must keep fibers aligned in the direction of loading to ensure maximum strength. Multiple fibers can be oriented in different directions to help support different loads.

One of the most important factors in creating strong composites is the matrix fiber bonding strength. This force can be tuned by careful material selection and surface treatments [68,69]. If the shear stress between the matrix material and the fiber exceeds the bonding strength, then the matrix will separate from the fibers, most likely leading to failure. Ideally, the matrix will transfer a load to the reinforcement fibers up to the ultimate tensile strength of the fibers, leading to a fiber failure.

2.10 Composite AM Technologies

One of the inherent benefits of layer based manufacturing in AM technologies is the ability to directly modify cross sections of a part during manufacturing. An example of such a

manipulation is operator selected infill patterns. Having the ability to discretely deposit material allows for optimization of material properties at the hand of the designer. A composite approach expands the design space further by allowing the designer to create multi material components. Several AM composite technologies have been explored including reinforced filaments, doped filaments, and ultrasonic/thermal embedding.

2.10.1 Reinforced Filaments

One composite material extrusion process uses fiber reinforced thermoplastic filaments to achieve high strength parts [70]. This method uses a continuous fiber composite technique with a thermoplastic matrix. The process works by extruding fiber reinforced filament through a heated nozzle similar to other material extrusion processes [71]. One interesting deviation from traditional composites is the introduction of filament strand boundaries in the matrix versus a continuous isotropic or laminate anisotropic matrix typically used in composites. This technique requires sufficient polymer bonding between the thermoplastic filament strands to transfer the shear load to the fibers without causing fractures in the matrix between strands.

2.10.2 Doped Filaments

Another material extrusion composite process is the use of doped filaments. Doped filaments combine particles or short fibers with a polymer matrix such as Acrylonitrile Butadiene Styrene (ABS) or Polylactic Acid (PLA). Many different dopants are used in filaments to achieve specific properties such as conductivity, illumination, and textures [72–75]. Mechanical properties of parts manufactured by material extrusion have also been altered by the introduction of dopants including an iron doped nylon filament for direct tooling [76], iron and copper doped ABS for higher stiffness and improved thermal conductivity [77], and carbon nanotube doped ABS filaments for higher stiffness and up to a 39% increase in yield strength [78].

2.10.3 Ultrasonic/Thermal Embedding

Embedding materials via thermal or ultrasonic techniques is a way to incorporate multiple materials in a manufacturing process. One example of this in AM is the thermal embedding of copper wire into material extrusion thermoplastic structures for improved conductivity and mechanical strength [79]. The process incorporates metals into the FFF process creating three dimensional structural electronic components.

2.10.4 Multifunctional and Tunable Materials

Multifunctional materials in AM were first presented through the integration of Vat Photopolymerization (VP) and Direct Write (DW) using conductive inks [80]. The idea of integrating VP and DW was aimed at creating structural components with embedded electronics, moving away from traditional structural shells with internal circuit boards and wire leads.

2.11 2D DIC Strain Analysis

Digital Image Correlation (DIC) is a full field measurement technique that compares digital images recorded throughout a material test to optically determine displacement and strain [81]. This technique has become popular in the experimental mechanics community since the 1980s as a non-contact measurement technique [82]. Technological advancements in microcomputers, image processing, cameras, optics, and DIC algorithms have made DIC a reliable alternative to traditional strain measurement techniques such as strain gauges [83]. A speckle pattern can be physically attached to the test surface via white a black paint [83].

CHAPTER 3
MANUFACTURING COMPOSITES USING A HYBRID MATERIAL EXTRUSION-
PHOTOPOLYMERIZATION METHOD

Modified from a paper to be published in
Emerald Insight Rapid Prototyping Journal

Ryan Hemphill, Douglas L. Van Bossuyt, Aaron Stebner

Abstract

The shift towards using low cost Additive Manufacturing (AM) processes including Fused-Filament Fabrication (FFF) and Stereolithography (SLA) for low production volume runs of end use parts has shown a need for versatile, high performance polymer AM materials. Limited material options for both FFF and SLA, and delamination failure modes of layer based components result in components that are not always suited for load bearing applications. A multi-material composite approach can provide components with desirable traits including higher ultimate strength, high specific strength, and appropriate stiffness for a specific application. In this article, we present the Fused Filament Fabrication-Stereolithography (F3SLA) process, a hybrid AM technique that incorporates both thermoplastic shells and liquid polymer infills. We present a case study aimed at exploring several multi-materials' suitability for load bearing applications and the effects of multi-material AM samples under both tension and compression. Our case study shows distinct benefits of 100% photopolymer infilled F3SLA components and a decrease in performance for photopolymer filled thermoplastic honeycomb infill. Development of F3SLA is a step towards achieving higher performance low cost polymer AM components.

Key Words: Additive Manufacturing, Photopolymer, Thermoplastic

3.1 Introduction

Additive Manufacturing (AM) has gained a tremendous amount of interest among engineers, scientists, and the maker community over the last decade. Several AM processes such as Fused Filament Fabrication (FFF) and Stereolithography (SLA) have recently become affordable for a broad range of applications and have spurred the rapid adoption of AM in many different industries such as aerospace, automotive, medical, and advanced manufacturing [2]. Driven by several factors including rapid low production volume part runs, no requirements for specialized tooling, and no complexity penalization for parts, AM is changing the way low production volume parts are manufactured [84]. In particular, layer-based manufacturing methods greatly reduce manufacturing costs associated with geometric complexity and therefore open up many new design possibilities that were previously cost-prohibitive or could not be physically built via subtractive machines (e.g.: computer numerical control mills, wire electrical discharge machining, lathes, etc.). However, the benefits of AM do not come without drawbacks and limitations. AM contains a whole new set of issues not typically present in subtractive manufacturing (SM) processes such as delamination failures, large internal stresses, and porosity [85].

FFF, or Fused Deposition Modeling³ (FDM) and SLA are the two most widely used AM methods for plastics due to the low cost and relative simplicity of the manufacturing processes [14]. A significant issue facing FFF and SLA for production run part adoption is the material properties of the printed parts [1]. Layer-based manufactured parts have a unique set of failure modes that are not generally found in SM parts and are more akin to failures found in composite materials [85]. Furthermore, mechanical properties of AM parts produced by economical

³ Registered trademark of Stratasys, Inc., Eden Prairie, MN; www.stratasys.com

commercial options are inconsistent across production runs due to process variations (e.g.: extruder temperature, ambient temperature, bed temperature, extrusion rate, print speed, etc.) [21]. Of particular interest to the research presented in this paper is tensile and compressive loading failures primarily manifested as delamination failures where the bonds between individual layers of plastic filament break at much lower yield strength than bulk material properties otherwise indicate [21]. Various methods to strengthen inter-layer bonding are available such as increasing extrusion nozzle temperature, decreasing layer height, elevating build volume temperature, and additional techniques primarily focused on increasing polymer chain interactions between layers [86]. Other methods of strengthening inter-layer bonding focus on infiltrating the printed part with a bonding agent such as an adhesive or using a solvent to promote additional interlayer bonding [16]. However, the tensile strength gains are still modest and do not equal or surpass bulk material properties.

While polymer AM process such as FDM and SLA can produce quality non-load bearing parts, there is a need for an alternative capable of producing economical load bearing-parts. In this paper, we present Fused Filament Fabrication-Stereolithography (F3SLA), a hybrid AM method combining elements from FFF and SLA, to increase polymer AM part mechanical strength, increase production speed of high infill prints, and expand material options for tunable polymers. It should be noted that we use the term “hybrid” as the combination of multiple AM process rather than the combination of AM and SM technologies as seen in [87–89]. F3SLA uses a FFF thermoplastic shell filled in up to 100% density with a liquid resin (e.g.: photopolymer, thermoset, epoxy, etc.). The resulting parts have the following beneficial properties: 1) wider range of available mechanical properties than FFF alone, 2) more rapid print completion than FFF with larger infill percentage, 3) less expensive equipment than SLA processes, and 4) theoretical

greater UV stability than SLA parts due to thermoplastic shielding. Relevant literature and the development and validation through tensile and compressive material testing are presented in the following sections.

3.2 Background

AM has gained popularity in the last decade due to several benefits including 1) eliminating costs associated with part complexity, 2) minimizing material waste, 3) increasing turnover rate for low production runs, and 4) eliminating tooling [2]. These benefits bring down manufacturing costs significantly and therefore result in a more streamlined, cost effective design and manufacturing process [90]. In addition to the reduction of costs, AM can produce part geometries not previously possible with SM due to the layer-based approach such as complex lattice structures or fully assembled internal components. One benefit that we believe has not been fully exploited by the AM community is the ability to construct composite parts. While we see multi-material approaches in use with features like dissolvable material and color printing, multi-material processes can also be used to achieve desirable mechanical properties as seen in composites [56]. F3SLA builds on several AM processes that were developed over the last 30 years and are widely available to industry and academia. This section reviews literature and information relevant to the hybrid FFF-SLA method presented in this paper.

3.2.1 AM Toolchain

The general AM toolchain includes Computer Aided Design (CAD), a slicer, host software, the AM machine, and post processing [10–12,91]. First, the part is designed for AM in CAD and saved as a mesh format such as a STL or Initial Graphics Exchange Specification (IGES) file. This file is converted into toolpaths via G-code using a slicer. The host software package can be installed on the printer itself or operated via an external computer. Host software loaded onto an external computer or AM microcontroller usually integrates the slicer and printer controller into

one package. Once the G-code has been generated, it is uploaded to the AM machine and the printing operations are carried out resulting in a geometrically finished part. Depending on the AM technology and specific application, post processing may be required to obtain a finished part. The AM toolchain simplifies the traditional SM toolchain by eliminating several time-consuming steps including drafting and tooling. A more detailed description of the general AM toolchain can be found in [16].

3.2.2 Fused Filament Fabrication

The FFF process is based on a thermoplastic filament fed through a heated extrusion nozzle at a controlled rate and deposited as a continuous feed of molten plastic at discrete locations on a build plate [20]. The build plate is often heated depending upon the specific system and thermoplastic being used. FFF uses a three axis platform typically actuated with stepper motors and an extruder assembly composed of a plastic filament driver and a hot end [10]. Most FFF implementations build parts, layer by layer, in the Z axis where the layer cross sections are in the XY plane [92]. Careful control of printing parameters allows complex geometries to be constructed. The two major manufacturing techniques that are used to produce a FFF part are shells and infill. Shells are the outermost layers that form the part's geometry while infill is the interior support for the shells that come in many different forms (rectilinear, conical, honeycomb, etc.). One major drawback to FFF is the large amount of time it takes to manufacture a part, especially for large parts and high infill percentages. High infill percentages help to increase strength of printed parts by providing more structural support. However, there is a tradeoff between build time and part strength as dictated by infill [21]. Some optimization of build time and part strength can be achieved through an advantageous build orientation aligning filament strands with application loads [93,94].

3.2.3 Stereolithography (SLA)

SLA uses photo-curable resins and a light source such as a laser or digital light processing⁴ (DLP) projector to cure each successive layer in a part [84]. Liquid photopolymer resin is selectively bombarded with focused light to cure the photopolymer to a solid state [30]. Typically, SLA uses a vat of photopolymer with a height-adjustable build plate that enables layer-based manufacturing. UV light is commonly used to cure the photopolymer in a layer pattern specified by the slicer software [95]. SLA uses a laser to trace each layer while a DLP SLA machine uses a digital projector to cure an entire layer at once, decreasing build time [33]. The SLA AM method also typically results in higher resolution parts than FFF. Material properties (e.g.: percent elongation, tensile/compressive strength, brittleness, etc.) vary greatly in SLA due to the large number of photopolymer blends available and inconsistent material properties among blends [96]. Disadvantages of SLA include UV stability, brittleness, warping, internal stresses and cure imperfections such as air pockets [29]. Some of these disadvantages can be mitigated through careful parameter tuning but others are material characteristics such as UV stability and brittleness [96].

3.2.4 AM Materials

Both FFF and SLA are limited by the materials suitable for each technique. FFF uses thermoplastics such as Polylactic Acid (PLA), Acrylonitrile Butadiene Styrene (ABS), High Impact Polystyrene (HIPS), and various polyamides (Nylons) [17,97]. These materials all vary in mechanical properties such as tensile strength, brittleness, and UV stability. Regardless of the variations in mechanical properties, almost all FFF materials are thermoplastics and therefore exhibit certain similarities such as relatively low melting temperatures. SLA materials also vary

⁴ Registered trademark of Texas Instruments, Inc., Dallas, TX; www.ti.com

widely but are all typically proprietary blends of photopolymers. Under light bombardment of a certain wavelength, depending on the photo initiators used, photopolymers undergo cross-linking polymerization.

3.2.5 Composites

Composites combine multiple materials to achieve desired material properties not feasible through the use of one bulk material [98]. Typically, this encompasses a support matrix such as an epoxy or ceramic reinforced with a phase material such as carbon fiber, fiberglass or metal fiber [99]. Since the fiber reinforcement acts to support the main load while the support matrix holds the entire part together, fiber orientation is extremely important [98]. There are many different techniques to manufacture composites from hand layup to semi-automated processes including Resin Transfer Molding (RTM), Resin Injection Molding (RIM), and Vacuum-Assisted Resin Transfer Molding (VARTM) [100–103]. Composite parts therefore also exhibit different failure modes than single-material parts [69,104]. Composite failure modes can be classified as a matrix failure where the bonding between the matrix and fiber fails or a phase failure where the fibers themselves fail [105,106]. This is more akin to AM part failures where failure typically occurs at layer boundaries.

3.2.6 Composite AM Technologies

The discrete deposition of material in AM technologies inherently enables the feasibility of complex multi-material components. We have classified composite FFF technologies into three categories including reinforced filaments, doped filaments, and ultrasonic/thermal embedding. One attempt at producing economical load bearing parts is the use of fiber reinforced thermoplastic filaments [70,107]. This process uses specially manufactured thermoplastics with a fiber-reinforced core composed of fiberglass, Kevlar, or carbon fiber and two extruders to allow the fiber-reinforced thermoplastic to be laid in orientations specified by the operator [107]. The fiber

reinforced filament process is limited to laying reinforcement in only the X-Y axis and therefore does not allow reinforcement between layers. Doping of filaments is another technique used to incorporate multiple materials in AM to achieve a desired set of material properties. Metals such as iron and copper along with carbon are often used as dopants in thermoplastic filaments to achieve a higher stiffness, increased thermal conductivity, and increased yield strength as seen in [77,108].

3.3 Development and Validation of F3SLA

The methodology presented below details F3SLA in two main subsections including development of F3SLA, and process validation through material testing. The benefits of F3SLA include a wider range of material properties and more rapid part completion. Tensile and compressive tests were used to evaluate the mechanical integrity of F3SLA components.

3.3.1 F3SLA Development

We began development of F3SLA by manually testing the printing procedure using a FFF machine to build the shell and thermoplastic infill structure, a syringe to manually insert photopolymer, and a handheld UV light for layer curing. This allowed us to quickly vary parameters in order to gain an understanding of the process before automation. Of particular interest was how a liquid matrix would interact with the solid AM thermoplastic shell including seepage and material reaction. Due to the propriety nature of commercial photopolymers, some initial experimentation was conducted to verify that PLA and the selected general purpose photopolymer would not react on contact or during curing [109].

After understanding how F3SLA can work by combining photopolymer and thermoplastic into a hybrid AM process, we proceeded to develop an automated AM printer to produce F3SLA parts. F3SLA is based on a thermoplastic shell, thermoplastic reinforcement, and photopolymer infill. We achieve this by expanding the FFF procedure to encompass more than just thermoplastic

extruders. Typically, multi-extruder thermoplastic FFF machines will vary filament color or filament material type. For instance, dissolvable support material is often loaded into one thermoplastic extruder while the other extruder contains the build material. Color FFF printers also usually incorporate multiple extruders with a distinct colored filament loaded in each extruder. The hybridization of FFF and SLA overcomes material limitations of each process resulting in a broader range of mechanical properties such as tensile strength, brittleness, UV stability, etc. The practical implementation of F3SLA differs from typical multi-extruder FFF printers, where identical thermoplastic extruders deposit one or more thermoplastics (e.g. MakerBot, MakerGear M2), by incorporating multiple material phases [110,111].

A F3SLA printer uses a standard FFF thermoplastic extruder for laying down the thermoplastic shells, and a stepper motor-driven peristaltic pump attached to a nozzle as the liquid photopolymer extruder. A UV light is also either included on the gantry assembly of the F3SLA printer or mounted stationary above to build platform to cure the photopolymer in layered intervals. Figure 3.1 shows one possible F3SLA print head setup.

For initial testing, we used a standard FFF printer for the initial development and testing of F3SLA. The FFF printer was used to create the shells and thermoplastic reinforcement while infill of the photopolymer was performed manually during the FFF printing process. We used an external computer to control pause points and gantry movements through custom g-code scripts in the build process to allow manual insertion of the photopolymer and UV curing. A standard medical syringe, as seen in Figure 3.2, was used for manual resin deposition while a handheld UV light was used for curing. We used PLA and a general purpose commercial UV photopolymer for initial testing and development of F3SLA. Theoretically, any liquid resin including various photopolymers, thermosets, and epoxies, can be used in place of photopolymers with F3SLA to

produce AM parts with different desirable material properties. The manual deposition process is shown in Figure 3.2 where the thermoplastic shell (black) can easily be distinguished from the liquid photopolymer infill (red).

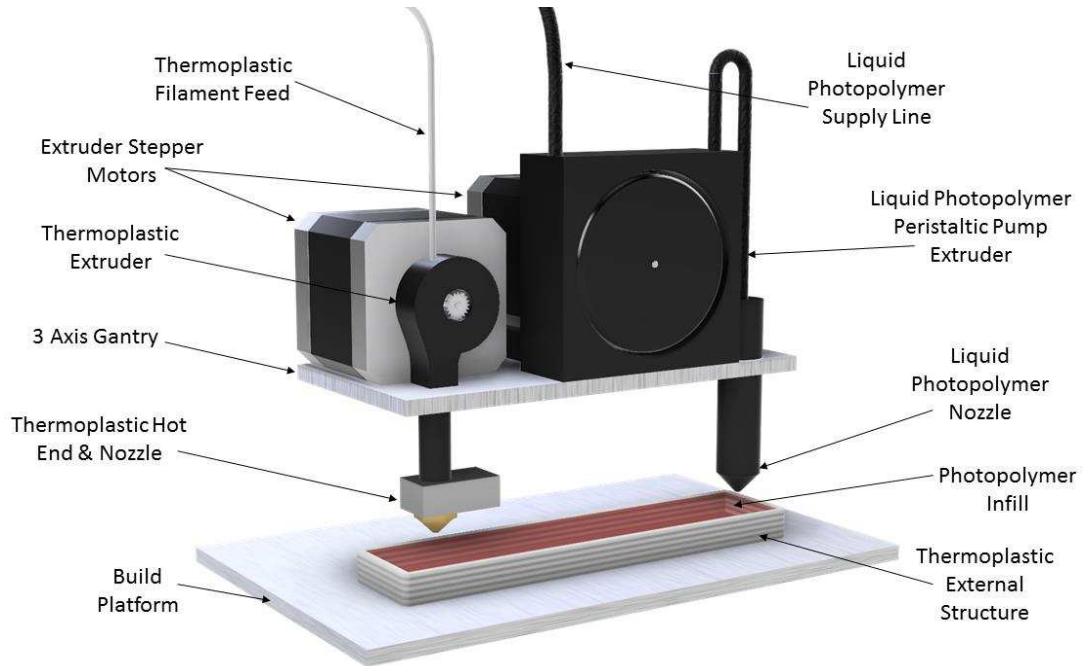


Figure 3.1: Possible F3SLA Gantry Setup

Manual F3SLA testing allowed us to successfully validate F3SLA on the basis of material compatibility, dimensional accuracy, and layer height. Due to the external thermoplastic shell providing geometric dimensional accuracy and surface finish, a larger photopolymer layer height is advantageous in decreasing build time. Figure 3.3 illustrates several issues with increased layer height including air bubbles, liftoff, and warping. In Figure 3.3, layer height decreases from left to right. Air bubbles can be seen in the two leftmost samples while some degree of liftoff can be seen in all but the rightmost sample. A slower cure time can decrease both liftoff and warping and can be achieved through less intensity, modification of wavelength for photopolymer curing, or decreasing exposure time. The rightmost sample indicates how ultra-thin layers can be achieved with minimal air bubbles, liftoff, and warpage. The layers shown in Figure 3.3 are the first

photopolymer layers of various heights therefore the ridges of the individual thermoplastic strands can be seen in the rightmost sample due to resin seepage between strands.



Figure 3.2: Manual Photopolymer Deposition Process



Figure 3.3: F3SLA Adhesion Tests

Thermoplastic reinforcement can be added to the F3SLA composite structures to minimize warpage, provide rigidity, and tune mechanical performance including yield strength, strain, and specific strength. Warpage, due to the exothermic photopolymer cure reaction, can be mitigated through thermoplastic reinforcement and an increase in build plate adhesion through the use of adhesives and/or elevated bed temperatures. Figure 3.4 shows several test samples with thermoplastic reinforcement showing complex geometries such as inclines and overhangs. FFF geometry limitations are shown in the F3SLA samples (Figure 3.4) such as high overhang angles yet these can be mitigated through the use of thermoplastic support material.



Figure 3.4: F3SLA Samples

3.3.2 F3SLA Validation

To validate the mechanical integrity of F3SLA components, we tested a variety of mechanical properties such as ultimate strength, specific strength, and strain under tension and compression loads. All test coupons were made in accordance to the American Society for Testing and Materials (ASTM) F2971-13 - Standard Practice for Reporting Data for Test Specimens Prepared by Additive Manufacturing [112] and ASTM D638-14 - Standard Test Method for Tensile Properties of Plastics [113] with minor modifications for our test setup. These modifications included reducing the overall length of tensile coupons to 5.5 inches by cutting both the clamp length and the reduced section to 1 inch in to maximize the number of test samples we could fit on the build plate in one orientation. The reduced cross section was left unmodified to stay as close to the ASTM standards as possible for our test setup. A type II style test coupon was chosen over a type I in order to promote failure within the reduced region as per ASTM D638-14 recommendations. We used a one inch cube for the compressive sample geometry because of the simplicity, ease of manufacture, and flat surface for accurate 2D DIC optical strain analysis.

All coupons were manufactured from HATCHBOX PLA filament (silver) [114] bought in the same purchase order and only unsealed directly before each print run to get similar bulk material properties. We used MakerJuice LABS G+ v5 3D printing resin [109] for our UV curable resin throughout the entire case study. This resin was chosen because it is a general purpose resin that is easy to work with and widely accessible. To evaluate F3SLA and determine the mechanical properties of interest for the test coupons (yield strength, strain, and percent elongation) both tensile tests and compressive tests were conducted. The interaction between photopolymer core and thermoplastic structure was of specific interest to this case study. In particular, we were interested in how the two materials' boundaries would interact and how much separation we would observe.

We used 2D DIC optical strain analysis for displacement acquisition and strain measurement throughout the tensile and compressive case studies. The optical approach allowed us to locally measure the strain across the testing region to fully investigate multi-material interaction and failures. Using a strain gauge would have just provided axial measurements and not the level of insight that 2D DIC local strain fields did. Ncorr [115], an open source DIC program, was used to perform DIC analysis on our tensile data. Images taken throughout the tensile and compressive loading of test coupons were processed by localized tracking of a black and white speckle pattern on each coupon. An in-depth description on how Ncorr works and the underlying theory is available [116]. Figure 3.5 shows a sample 2D DIC strain field overlain on a 100% photopolymer coupon produced through DLP. A complete set of 2D overlain strain field images can be found in [117].

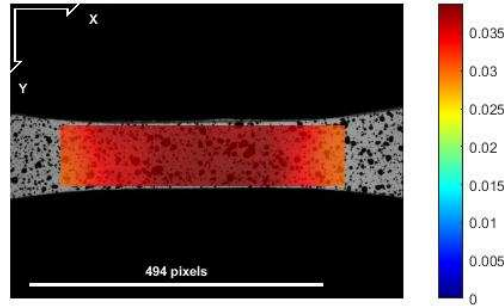


Figure 3.5: Sample 2D DIC Strain Field Overlay (100% DLP)

To perform DIC analysis during testing, we prepared samples by speckling the testing region. This process started with a light coat of white paint to provide a smooth, flat background. It was important to sufficiently coat the testing region to a point where the individual filament strands were not visible yet thin enough to minimize impact on the mechanical properties of the coupon. The second part of speckling involved misting the coupons with a black paint to a near 50-50 black and white balance. A consistent coating method was used throughout our tests to ensure accurate comparisons.

Table 3.1 presents an overview of the entire case study including both tensile and compressive sample cases. F3SLA samples were manufactured using a FFF process and manual photopolymer infill process as shown in Figure 3.2. All F3SLA samples used honeycomb thermoplastic infill structures.

Uniaxial tension and compression tests were used to measure material characteristics of both control cases and F3SLA cases and provide quantitative comparisons (ultimate strength, specific strength, strain, etc.) for evaluating the mechanical integrity and material characteristic flexibility of each case. A Mark-10 [118] ESM1500 single-column force tester was used for all material testing including both tension and compression tests. Two Mark-10 force sensors were used for tension and compression tests; a MR01-500 (500 lbf force limit) for tension and a MR01-2000 (2000 lbf force limit) for compression. Self-tightening wedge grips (Mark-10) were used for

all tensile tests while compression plates were used for compression tests. All tests were conducted at a constant displacement rate of 5 mm/s. A Basler [119] acA645-100gm GigE camera with 659 x 494 pixel resolution and a frame rate of 10 hertz was used for optical strain measurement. This resolution gave approximately 500 pixels for the testing region of both tensile and compression samples. Additional image settings and external fiber optical lighting intensity (aperture, gain, etc.) were individually selected for each case to provide an optimal image quality depending on environmental lighting and subtle differences in speckle patterns between sample cases.

Table 0.1: F3SLA Case Study Overview

Sample Process	Loading	Shell Material	Thermoplastic Infill (%)	Photopolymer Infill (%)
FFF	Tensile	Thermoplastic	0	0
FFF	Tensile	Thermoplastic	10	0
FFF	Tensile	Thermoplastic	20	0
FFF	Tensile	Thermoplastic	50	0
FFF	Tensile	Thermoplastic	100	0
DLP	Tensile	N/A	0	100
F3SLA	Tensile	Thermoplastic	0	100
F3SLA	Tensile	Thermoplastic	10	90
F3SLA	Tensile	Thermoplastic	20	80
FFF	Compressive	Thermoplastic	0	0
FFF	Compressive	Thermoplastic	10	0
FFF	Compressive	Thermoplastic	100	0
DLP	Compressive	N/A	0	100
F3SLA	Compressive	Thermoplastic	0	100
F3SLA	Compressive	Thermoplastic	10	90

Eight samples of each case were tested for both tension and compression. Figure 3.6 shows the geometry and dimensions for the tensile coupons in millimeters. A 1 inch cube block was used for the compression geometry to provide a flat surface for accurate optical strain measurement. The outer shell of all F3SLA samples were solid infilled (rectilinear FFF) PLA.

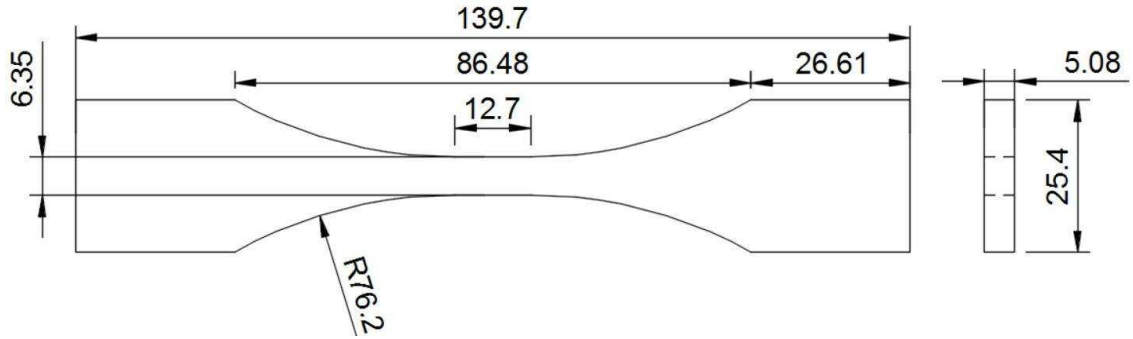


Figure 3.6: Tensile Coupon Geometry (mm)

3.4 Experimental Results

We present F3SLA material testing results in the following three subsections: tensile test results in Section 3.5.1, compressive test results in Section 3.5.2, and a summary of all results in section 3.5.3. All stress-strain plots report median stress-strain curves while the case study overview, Table 3.2, presents mean values to provide a more complete picture of the true central tendency of the data.

3.4.1 Tensile Data

We present the results of the FFF tensile control cases in a median stress-strain plot shown Figure 3.6. The FFF samples of various infill densities all followed a clear trend of increasing both ultimate tensile strength and stiffness with an increase in infill density. FFF honeycomb infill densities of 0%, 10%, and 20% all exhibited a median ultimate strength within 3% of each other. A 50% infill density coupon resulted in a 13% increase in strength over a 20% infill density coupon while a 100% infilled coupon resulted in a 47% increase in ultimate strength over a 50% infilled coupon. 100% Photopolymer coupons manufactured by DLP exhibited an 8% lower ultimate strength than 0% infilled thermoplastic manufactured by FFF and a similar stiffness to 10% or 20% infill density FFF samples.

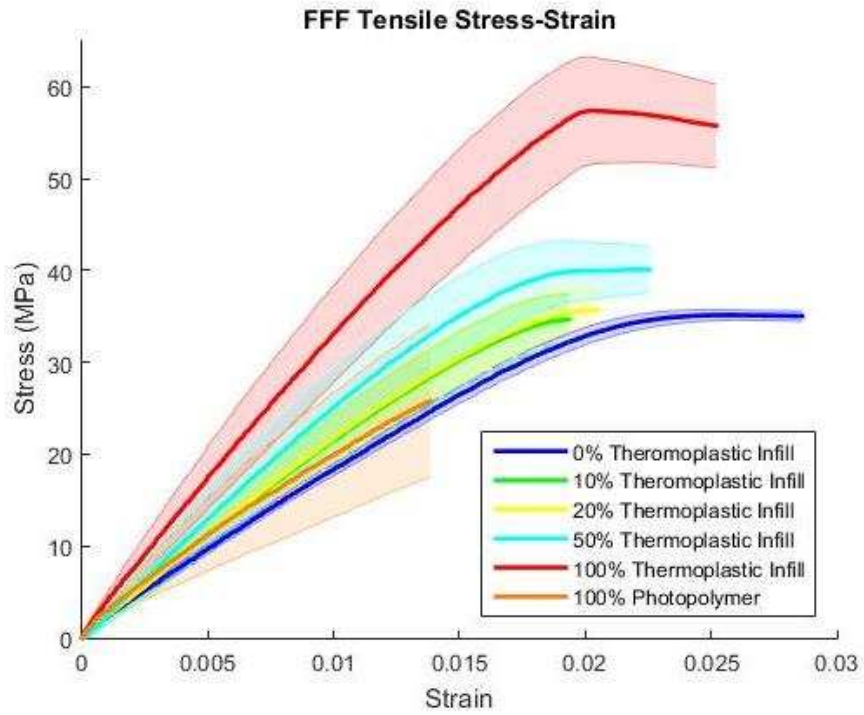


Figure 3.7: Control Stress-Strain Curves

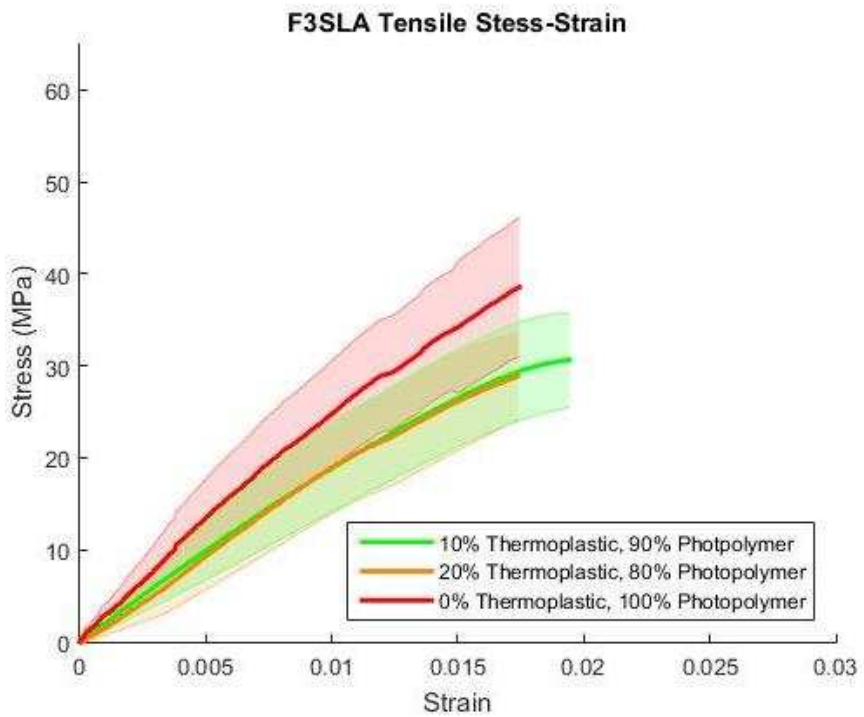


Figure 3.8: F3SLA Stress-Strain Curves

The F3SLA tensile stress-strain curves for photopolymer infilled thermoplastic honeycomb infill coupons are presented in Figure 3.7. The 10% F3SLA sample exhibited a 2% decrease in ultimate strength and the 20% F3SLA case exhibited a 6% increase in ultimate strength over the DLP control case. The 0% F3SLA sample resulted in a 45% increase in ultimate strength over the DLP control case. The 0% F3SLA case resulted in a 34% increase over 0% thermoplastic FFF case but a 27% decrease versus 100% thermoplastic FFF case.

3.4.2 Compressive Data

The compressive stress-strain curves for the FFF and DLP control cases are presented in Figure 8. Due to load frame limitations, not all compressive cases were loaded to failure. Failed cases are indicated in Table 3.2. Figure 3.9 shows the results of the F3SLA samples under compression.

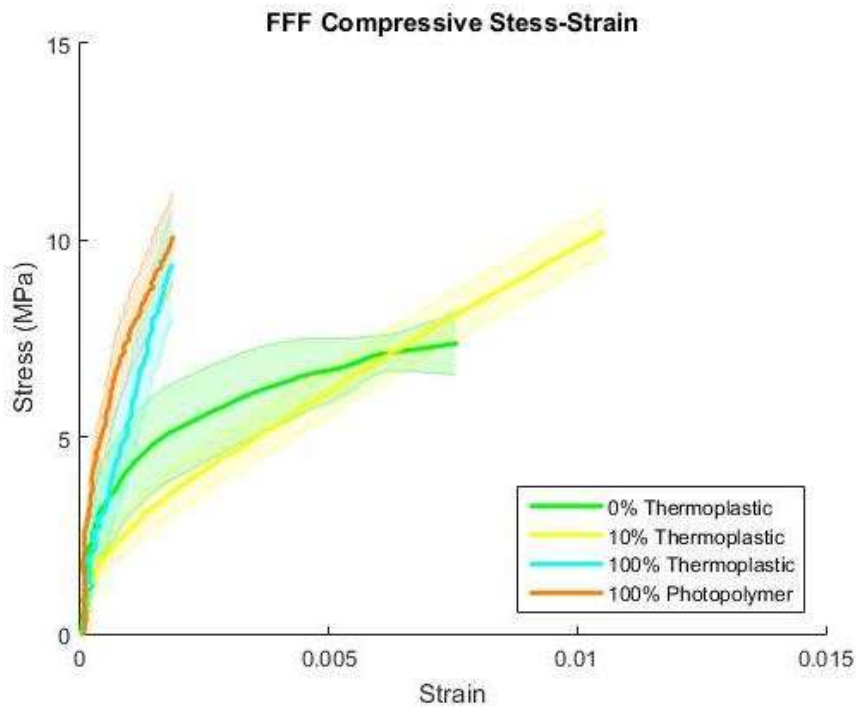


Figure 3.9: Control Compressive (-) Stress-Strain Curves

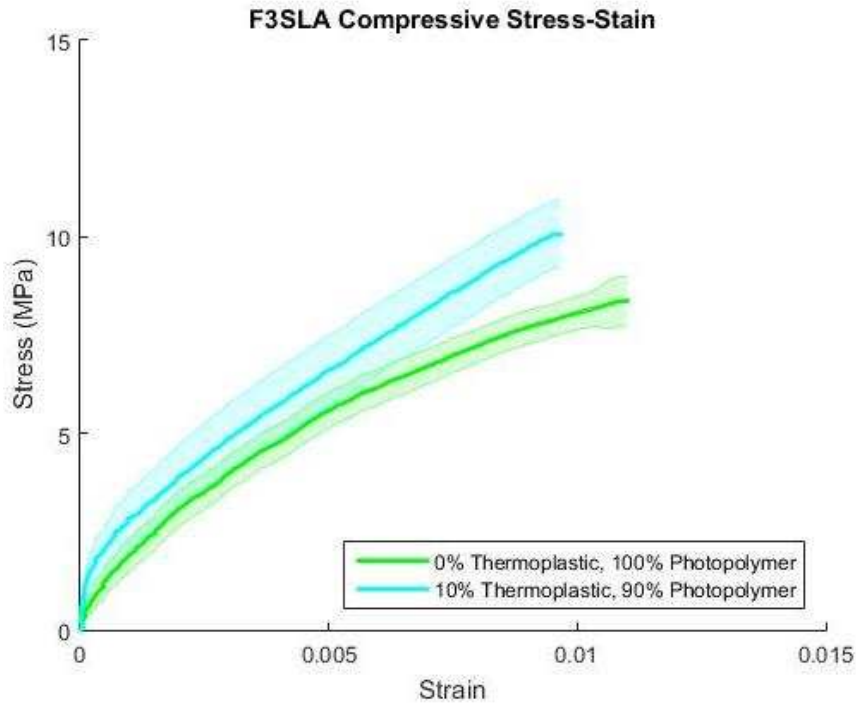


Figure 3.10: F3SLA Compressive (-) Stress-Strain Curves

3.4.3 Summary

A complete summary of the F3SLA case study is presented in Table 3.2. It should be noted that not all compressive samples were loaded to failure due to load frame limitations. All failed samples are indicated in the case study overview. Young’s Modulus was calculated as the tangent modulus for the linear elastic region of each sample case. This was achieved by manually selecting the linear region for each case and averaging the results across all eight samples. Note that the cases largely exhibit nonlinear responses and therefore the Young’s modulus is only a valid measurement of material compliance within the linear elastic region.

Table 3.2: F3SLA Case Study Results Summary

Sample	Load	Fail	Ultimate Stress (MPa)	Ultimate Stress Std Dev	Ultimate Strain	Strain Std Dev	Youngs Modulus (Mpa)	Effective Specific Strength (kPa/kg/m ³)
0% Thermoplastic Infill (FFF)	T	Yes	35.18	0.434	0.0267	0.0008	1747	61.26

Table 3.2 Continued

Sample	L o a d	Fail	Ultimate Stress (MPa)	Ultimate Stress Std Dev	Ultimate Strain	Strain Std Dev	Youngs Modulus (Mpa)	Effective Specific Strength (kPa/kg/m ³)
10% Thermoplastic Infill (FFF)	T	Yes	35.17	0.732	0.0215	0.0022	2195	51.81
20% Thermoplastic Infill (FFF)	T	Yes	36.06	0.496	0.0231	0.0011	2193	47.30
50% Thermoplastic Infill (FFF)	T	Yes	40.67	0.485	0.0236	0.0013	2555	41.88
100% Thermoplastic Infill (FFF)	T	Yes	60.28	1.710	0.0236	0.0016	3341	49.76
100% Photopolymer (DLP)	T	Yes	30.80	4.899	0.0213	0.0080	1978	23.04
10% Thermoplastic , 90% Photopolymer (F3SLA)	T	Yes	31.90	1.268	0.0235	0.0014	1952	35.52
20% Thermoplastic , 80% Photopolymer (F3SLA)	T	Yes	34.06	2.439	0.0258	0.0021	1739	35.07
0% Thermoplastic , 100% Photopolymer (F3SLA)	T	Yes	45.18	7.364	0.0275	0.0069	2789	44.60
0% Thermoplastic Infill (FFF)	C	Yes	7.46	0.224	0.0061	0.0021	11972	61.26
10% Thermoplastic Infill (FFF)	C	No	N/A	N/A	N/A	N/A	6178	N/A
100% Thermoplastic Infill (FFF)	C	No	N/A	N/A	N/A	N/A	9636	N/A
100% Photopolymer (DLP)	C	No	N/A	N/A	N/A	N/A	13557	N/A

Table 3.2 Continued

Sample	Load	Fail	Ultimate Stress (MPa)	Ultimate Stress Std Dev	Ultimate Strain	Strain Std Dev	Youngs Modulus (Mpa)	Effective Specific Strength (kPa/kg/m ³)
0% Thermoplastic, 100% Photopolymer (F3SLA)	C	Yes	8.55	0.61	0.0108	0.0041	3028	8.62
10% Thermoplastic, 90% Photopolymer (F3SLA)	C	No	N/A	N/A	N/A	N/A	8857	N/A

3.5 Discussion

The following discussion highlights our interpretations of the data trends presented in Section 3.4. We explore the mechanical integrity of HATCHBOX PLA and MakerJuice G+ photopolymer and their possible use for load bearing parts. We then discuss F3SLA’s potential versus FFF and DLP.

The motivation for exploring various thermoplastic and photopolymer infill density combinations was to use the thermoplastic as the phase material and photopolymer as the matrix material of a F3SLA composite. We saw an opposite effect with a lower ultimate strength in the 10% and 20% F3SLA cases versus the corresponding 10% and 20% FFF cases. Examining the test specimens, we attribute this decrease in performance to the introduction of defects (e.g.: poor layer bonding, air pockets) into the test coupons. Thermoplastic does not bond well to the smooth surface finish of cured photopolymers. Significant seepage would also have to occur for the liquid infill to form a continuous matrix. Based upon optical observations, we suspect that the individual pockets of photopolymer did not seep through and successfully crosslink with neighboring pockets.

The 15% increase in ultimate strength from the 0% Thermoplastic-100% Photopolymer case versus the 50% infill density FFF case suggests that F3SLA has potential to provide high strength parts at lower build durations than high thermoplastic infill densities. While the 100% infilled thermoplastic case still out-performs all F3SLA cases in terms of ultimate strength and specific strength, the potential decrease in build time can be attractive for certain applications such as load-bearing prototypes, and end-use components that don't require higher performance. These applications will value quick manufacturing turnaround and high quality surface finish [120] over strength.

From the 96% increase in ultimate strength and 116% increase in specific strength, it is clear that the photopolymer used is not as strong of a material as the thermoplastic used under tension. This explains the 33% increase in ultimate strength between the 0% Thermoplastic-100%Photopolymer F3SLA case and the 100% thermoplastic FFF case.

From these comparisons, it is clear that the photopolymer chosen (under the curing parameters as defined by the manufacturer [121]) is a much weaker material than the PLA used when looking at both ultimate strength and specific strength. The DLP case also exhibited a much larger standard deviation in ultimate strength than the samples produced through FFF. We believe this is due to the brittleness of photopolymer and therefore there is a large chance of defect propagation. Minor defects have a greater chance of leading to ultimate failure of a component made out of photopolymer than more durable thermoplastics.

To evaluate the F3SLA process in direct comparison to both FFF and DLP we split the material testing case study results into three groups including coupons produced by FFF, DLP, and F3SLA. Each coupon group was evaluated on several metrics including ultimate strength, specific strength, stiffness, and repeatability. We recommend processes that resulted in above average

performance in Table 3.3. Note that these processes are evaluated on a limited number of materials including HATCHBOX PLA (silver) and MakerJuice G+ (red). A larger dataset including more compatible materials will provide a better generalization than presented in Table 3 and should be constructed before widespread adoption of F3SLA.

Table 3.3: Process Recommendation for Various Parameters

Desired Parameter	Process Recommendation
Ultimate Strength	FFF, F3SLA
Specific Strength	FFF, F3SLA
Stiffer	FFF
More Compliant	F3SLA, DLP
Repeatable	FFF

3.6 Future Work

While this research has laid the foundations of F3SLA, more cases, catalogued data, and a toolset are needed to develop the process into a reliable manufacturing method. The characterization of various thermoplastics, photopolymers, and other thermosets will be key to successful implementation in industry. Material choice will also be an important factor to be researched and developed. We chose an easy to obtain, general purpose, non-toxic photopolymer although better choices for mechanical integrity are likely available.

F3SLAs liquid photo polymer deposition allows for the possibility of fiber to be inlaid. The combination of thermoplastic framework, liquid photo curable resins, and fiber would allow true composites to be manufactured using AM. Theoretically we could then use any combination of reinforcement fibers (e.g.: carbon fiber, Kevlar, etc.). A fiber inlay case study should be conducted to determine the effectiveness of reinforced F3SLA components.

Different curing techniques for liquid polymers should also be explored. We chose UV photo curable materials due to the speed and amount of control we have over curing. It may be possible to exploit other curing methods such as two part epoxies. This addition would further

expand the printable material bank and therefore give people even more control over tunable parameters.

3.7 Conclusion

F3SLA is a first step towards directly manufacturable low-cost composites through AM techniques. We found F3SLA to be a viable option with many directions for future development. Our initial test runs have successfully produced samples of several geometries. A set of suitable printing parameters were identified through process iterations and are ready to be incorporated in an automated process [117]. F3SLA brings new possibilities to the field of AM by incorporating a wide range of materials in one process. While the framework for this method has been laid out, much more work is needed to bring this method to industry and the maker community. The first research phase presented here incorporated many parameter iterations making large data samples unfeasible. Future work will be needed to expand data sets and catalogue material mechanical properties to verify process robustness and provide a database for component design.

Although photopolymer infilled thermoplastic honeycomb samples were not successful in achieving a higher ultimate strength or specific strength, 100% infilled F3SLA samples did show potential. The 100% infilled photopolymer sample exhibited a 45% increase over 100% photopolymer samples produced by DLP and a 15% increase in ultimate strength over 50% infill density thermoplastics produced by FFF.

There are many potential applications for a fully developed F3SLA. Industries such as aerospace and automotive already utilize AM due to its unique ability to manufacture complex geometries simply not feasible using subtractive methods. The addition of mechanically reliable low cost AM polymers opens up a whole new field of parts for AM to produce both for industry and for hobbyists.

CHAPTER 4
DEVELOPMENT AND VALIDATION OF AN ECONOMICAL POLYMER FIBER-
REINFORCED COMPOSITE ADDITIVE

Modified from a paper to be published in
Elsevier Additive Manufacturing

Ryan Hemphill, Douglas L. Van Bossuyt, Aaron Stebner

Abstract

The adoption of Additive Manufacturing (AM) for low production volume part runs has highlighted the need for more versatile AM materials to aid engineers, students, enthusiasts, and the maker community in designing high performance end-use components. Current low cost AM processes (e.g.: material extrusion and vat photopolymerization) have limited material choices that are not always suitable for use in load-bearing components. A composite material approach to AM can improve mechanical properties of components by combining multiple materials thus attaining the beneficial material properties of each separate material in an AM-produced composite. In this article, we present the development and validation of a composite AM process, the Reinforced Fused Filament Fabrication-Stereolithography (RF3SLA) process, through multiple material testing case studies. Throughout the validation of RF3SLA, we explore variations in matrix material and fiber reinforcement. 2D localized strain analysis is presented via digital image correlation to analyze F3SLA coupon failures, multi-material interactions, and fiber reinforcement effectiveness. Our material testing shows distinct differences in samples produced from the same two or three materials (thermoplastics, photopolymers, epoxies, and fibers), and highlights how mechanical property improvement can be achieved through tuning the design of composite AM materials given geometric constraints and desired component parameters (e.g.: strength, specific strength, stiffness, etc.). Implementation of the RF3SLA process is a step towards achieving tunable material properties for low-cost AM technologies.

Key Words: Additive Manufacturing, Composites, Photopolymer, Thermoplastic, Fiber-Reinforced Plastic

4.1 Introduction

Recent changes in Additive Manufacturing (AM) such as the introduction of affordable microcontrollers, expired patents that previously restricted commercial competition in machine and process development, and an increase in public interest have resulted in what some are calling the third industrial revolution [122]. While only time will tell if current trends towards a global maker community will have as large of an impact on global manufacturing as some are predicting, there is little doubt that AM is a disruptive technology [16,123]. Several major factors have led to the use of AM for rapid prototyping and low production run manufacturing. These factors include: 1) the widespread availability of low cost AM machines including material extrusion and vat photopolymerization, online businesses focused on economical quick turnaround manufacturing of AM parts, and community funding of projects [2–4]. While economical AM has helped to streamline the design process and provided a rapid and relatively inexpensive option for prototyping, the use of AM for end use parts is still in its infancy [1]. AM machine yield rates and predictable material properties are two primary barriers to the broad adoption of AM parts for production [21].

Public interest in AM has greatly increased in the last decade due in part to the promise of manufacturing parts at home with the click of a button. Printing products at home interests the public because it brings rapid access to products to a whole new level, theoretically allowing online shoppers to receive purchased goods almost instantaneously and without having to leave the home [5]. The technical community including engineers, scientists, manufacturers, and hobbyists see AM as a design tool, prototyping tool, and low production run manufacturing tool [6]. Mass

customization of parts and products is a key benefit of AM for both the public and the technical community due to AM's unique suitability for low production runs. Personalized goods such as unique colors, patterns, engravings, textures, and geometries are limited in mass production by factors such as the number of production lines constructed and tooling costs [7]. AM overcomes traditional mass production customization limitations by allowing the manufacture of a wide range of parts and products on a single production line without retooling costs[8].

The layer-based manufacturing approach seen in many AM processes is suitable for multi-functional materials and tunable material parameters due to discrete deposition or curing/sintering of feedstock material. The underlying idea of both multi-functional materials and tunable material parameters for parts is geometrical and material property customization of both external and internal part structures. Multi-functional materials have the potential for further miniaturization and increased performance of products through the integration of electronics, electrical pathways, thermal vias, and complex internal lattice structures into product casings [79,124]. The integration of electronics, thermal management, and structural optimization features provides a shift away from traditional design methodology where external casings, electronics, wiring, and thermal management are designed separately to fully integrated multi-functional components.

In this paper, we propose an economical composite AM technique, the Reinforced Fused Filament Fabrication-Stereolithography (RF3SLA) process, to achieve improved mechanical integrity and material flexibility for low cost polymer AM. To our knowledge, the RF3SLA process and our approach to producing parts with tunable material properties for specific applications is unique and novel in low cost polymer AM. Further, we present material testing data demonstrating how material properties can be tuned in RF3SLA to achieve desired part performance. The hobbyist and maker community can immediately benefit from RF3SLA by

implementing the process on hobbyist AM machines. We expect RF3SLA and related processes to become available to engineers and AM service houses in the near future as commercial machines are developed using the RF3SLA method presented here⁵.

4.2 Background

In this section, we briefly review two of the seven categories of Additive Manufacturing (AM) as defined by the ASTM F42 – Additive Manufacturing Committee [9] which include: Material Extrusion, Vat Photopolymerization, Binder Jetting [16,33–36,49], Material Jetting [16,38–40], Powder Bed Fusion [16,41–45], Directed Energy Deposition [16,46–48], and Sheet Lamination [49–52]. Of these seven AM categories, currently commercially available economically-priced options for engineers, hobbyists, and the maker community are Material Extrusion and Vat Photopolymerization machines. Material Extrusion and Vat Photopolymerization are of specific interest to the RF3SLA process and are examined in detail below. While costs are steadily decreasing for several other AM technologies including Binder Jetting and Material Jetting, there currently are no commercial machines marketed towards price-sensitive individuals and companies. We then survey relevant literature on several topics necessary to understand the RF3SLA process presented in this paper including: 1) the AM toolchain, 2) composite materials, and 3) related efforts to develop composite AM materials.

4.2.1 Material Extrusion

Material extrusion is the most common AM method in use today due to its widespread adoption in desktop 3D printers [14]. The basic principle behind material extrusion is the deposition of a material through a nozzle at discrete locations in a build volume [15]. For this AM process to work, material extrusion machines require at least three axes of motion, a material that

⁵ The Colorado School of Mines has filed a patent on the RF3SLA process.

can flow through a nozzle, and control over the flow of material [15]. Material extrusion typically requires four actuators for a single extruder setup to achieve three axes of motion plus one axis of extrusion. We have observed material extrusion's popularity coming from low barrier to entry, ease of use, relatively simple control strategies, and stable, safe feedstock materials.

Fused Filament Fabrication (FFF), or Fused Deposition Modeling⁶ (FDM) [15], is a common material extrusion method primarily found in inexpensive hobbyist and prototyping AM machines. FFF extrudes polymer filaments through a "hot end" that heats a thermoplastic filament past the filament's glass transition temperature, allowing the filament to flow through the nozzle when advanced by an actuator. The extruder assembly is typically mounted on a three axis gantry to lay down material according to a predefined toolpath. The toolpath is generated by a slicer program that imports 3D CAD geometry, slices the object into 2D cross sections, determines a toolpath to fill each cross section based on user preferences, and exports the toolpath in the form of g-code to the AM machine [16].

FFF machines typically use thermoplastics as feedstock for creating parts due to the relatively low glass transition temperature of thermoplastics and beneficial mechanical characteristics including strength and ductility [17]. Thermoplastics are commonly used in other manufacturing processes such as injection molding and vacuum forming [18,19]. However, parts manufactured via FFF exhibit anisotropic mechanical properties not often found in traditional manufacturing processes [20]. Due to the anisotropic nature of FFF parts, real-world mechanical properties usually fall well below bulk material properties [21]. Thermoplastics also exhibit mechanical property degradation at every recycling phase [22]. This both limits the reuse of

⁶ Registered trademark of Stratasys, Inc., Eden Prairie, MN; www.stratasys.com

feedstock and adds a layer of complexity to predicting thermoplastic mechanical properties in design.

4.2.2 Vat Photopolymerization

Vat Photopolymerization (VP) is a group of AM technologies that use photopolymers and a light source to cure successive layers resulting in 3D printed parts. The two commonly used AM VP technologies are Stereolithography (SLA) and a modified SLA technique using Direct Light Processing⁷ (DLP) [23,24]. Photopolymers are cured via the photo polymerization process usually initiated by ultra violet (UV) light in both SLA and DLP [16,25].

Two common machine configurations exist for VP including “top down” and “bottom up” machines [24]. The top down configuration uses a large photopolymer tank and a platform that is lowered into the tank. In this setup, the top layer of the part is cured first while the build platform is then lowered for each successive layer to be cured to the previous layer. The bottom up configuration cures the bottom layer first and raises the build platform up for each successive layer until reaching the top layer. Bottom up can use a much shallower photopolymer tank as only a layer height of photopolymer theoretically needs to be in the tank for each layer. VP processes typically achieve the best accuracy and surface finish across all AM techniques [16].

SLA VP uses photopolymers to successively build up layers into a finished 3D part. A laser beam is used to cure the photopolymer in a 1D channel approach where only one discrete point is photoset at a time. A fixed laser is aimed at a scanning galvanometer that focuses the laser at discrete locations on the build platform. If there is liquid photopolymer between the beam and the build plate, it is cured by the laser. Tracing the cross section of the part at each layer cures the photopolymer into the correct cross sectional pattern, creating a cured layer [16].

⁷ Registered trademark of Texas Instruments, Inc., Dallas, TX; www.ti.com

DLP additive manufacturing uses a 2D channel approach that cures an entire layer at the same time. This is achieved by a DLP chip found in most modern digital projectors [16]. The process works by flashing cross sectional patterns of light of each successive layer at the build plate. Before each image is projected, the build plate is advanced, allowing the next layer to build directly on the previous. The benefits of the DLP SLA system are reduction in build time, simple mechanicals and software, and high resolution for small parts [27].

There are several important issues with photopolymer processes including: 1) shrinkage that occurs during curing [28], 2) poor and volatile mechanical properties [29], and 3) differences in crosslinked photopolymers and linear branched polymer changes [30]. Shrinkage arises from monomers taking up more volume than their cured polymer counterparts [16]. Curling of individual layers introduces internal stress in a part and can lead to inaccurate part geometry. To mitigate curling, a larger build plate bonding force can be used. We have found this can be achieved in multiple ways such as a rougher surface finish or cure time adjustment. Mechanical properties of photopolymers are less than desirable and volatile. This is due to several issues such as UV stability, brittleness, interlayer bonding due to uncured photopolymer, warping, and imperfections due to curing reactions such as air pockets, internal thermal stresses, and humidity [29]. Furthermore, mechanical properties of photopolymers directly depend on the mixture of monomers, photoinitiators, diluents, flexibilizers, and stabilizers [16]. Even if each specific blend of photopolymer is tested and cataloged, we have observed that variations in cure times or light intensities can still cause inconsistent mechanical properties. When photopolymers are bombarded by light waves with a specific wavelength-dependent photoinitiator (typically UV), polymerization occurs [30]. This chemical process cross-links monomer chains into larger polymer molecules

[30]. Cross-linked polymers differ from linear and branched polymer chains, such as those that make up thermoplastics, because they cannot be remelted and recycled [31].

4.2.3 AM Toolchain

The polymer AM toolchain begins with the modeling of a 3D part in a CAD environment. Once modeled, the CAD file is exported as a file that can be interpreted by slicer software. The most commonly used file type is the stereolithography (STL) format although other options do exist (e.g.: IGES, AMF, etc.) [10–12]. The slicer software generates 2D cross sectional slices of the 3D part and then generates a toolpath to fill each cross section via a layer-based approach [12]. The toolpath is then exported as g-code and uploaded to the AM machine controller. The controller can then execute the toolpath to print the 3D part.

4.2.4 Composites

Composites use multiple materials to achieve a desired set of properties including strength, strain, chemical resistance, strength/weight ratio, etc. Composites are made up of a continuous matrix material and various embedded reinforcement materials, or dispersed phases (e.g.: Glass, Carbon, Kevlar, Metallic, etc.) [53]. Fiber Reinforced Polymers (FRP) are one subset of composites that use various polymers as the matrix material [54]. FRPs originally were constructed from polymeric resins reinforced with glass fibers to achieve high strength, stiffness, and chemical resistance while maintaining low cost and weight [54]. Today there are many different FRP combinations including thermoplastics, thermosets, and photopolymers for matrix materials and glass, Kevlar, carbon fiber, etc. for reinforcement [55]. Matrix and reinforcement combination can be customized for specific individual applications.

Many composite manufacturing processes typically result in bulk material properties that are isotropic due to a near-random distribution of material units on a molecular scale [56]. Fibers have uniaxial aligned molecular units giving them uniaxial mechanical properties [56].

Composites take advantage of the high strength in one direction of fibers by orienting fibers in the direction of anticipated loading. Fiber reinforcement of composites includes three main categories including short fibers, long fibers, and global fibers [55].

Short Fiber Reinforced Polymers (SFRP) use a distribution of short reinforcement fibers embedded in the matrix to provide localized reinforcement. SFRP material properties depend on two main parameters including the fiber length distribution and the fiber orientation distribution [57]. Short fiber reinforcement is often used in injection molding and many different methods for determining and/or predicting fiber orientation exist including models and experimental approaches [58,59]. Typically, SFRP materials exhibit anisotropic material properties due to a majority of fibers aligning along the flow direction of the matrix material [60]. The critical fiber length is the length of fiber needed to obtain an effective mechanical property benefit (e.g.: higher strength, lower strain) [61]. This factor has been shown to increase with matrix temperature [62].

Long Fiber Reinforced Polymers (LFRP) are similar to SFRPs with one key difference: longer fibers. Fiber lengths of 6.35 mm (0.25 inch) or greater typically result in composites being classified as LFRP although this distinction is somewhat arbitrary [63]. LFRP composites have gained popularity in many industries (e.g.: aerospace, automotive) because of their distinct mechanical properties (primarily strength/weight ratio) and ability to be processed in existing manufacturing process (e.g.: injection molding) [64]. Fiber length is not the sole parameter to optimize when designing a composite as it is also important to look at orientation, shear strength of the matrix, surface finish of the fibers [64].

Global Fiber Reinforced Polymers (GFRP), also known as Continuous Fiber Reinforced Polymers (CFRP), use identical matrix and phase materials to SFRP and LFRP but use longer fibers [65]. As with the distinction between SFRT and LFRT composites, the distinction between

LFRT and CFRT is not clearly defined. CFRP composites are useful for specific material properties (e.g.: high strength, high impact resistance, etc.) although CFRPs are more difficult to manufacture than SFRT and LFRTs [65].

FRP composite failures are classified into two different categories including: 1) matrix failure and 2) fiber failure [66]. The simplest approach at predicting composite failures is to assume the fiber can support the matrix past the matrix's yield strength, therefore only taking into account the strength of the fibers when predicting tensile failure [67]. This is not physically the case in many instances, and therefore more accurate models that look at both matrix fiber bonding forces and fiber strength as separate failure cases have been developed [66]. A composite matrix transfers tensile load to reinforcement fibers via shear stress [56]. Additionally, the matrix must keep fibers aligned in the direction of loading to ensure maximum strength. One of the most important factors in creating strong composites is the matrix fiber bonding strength. This force can be tuned by careful material selection of constituent materials and surface treatments [68,69]. If the shear stress between the matrix material and the fiber exceeds the bonding strength, then the matrix will separate from the fibers and most likely will lead to failure of the composite under tensile load. Ideally, the matrix transfers a load to the reinforcement fibers up to the ultimate tensile strength of the fibers, leading to a fiber failure.

4.2.5 Composite AM Technologies

One of the inherent benefits of layer-based manufacturing in AM technologies is the ability to directly manipulate cross sections of a part during manufacturing. An example of such a manipulation is operator-selected infill patterns. Having the ability to discretely deposit material allows for optimization of material properties at the hand of the designer. A composite material approach to AM expands the design space further by allowing the designer to create multi-material

composite components. Several AM composite technologies have previously been developed including reinforced filaments, doped filaments, and ultrasonic/thermal embedding.

One composite material extrusion process uses fiber-reinforced thermoplastic filaments to achieve high strength parts [70]. This method uses a continuous fiber composite technique with a thermoplastic matrix. The process works by extruding fiber-reinforced filament through a heated nozzle similar to other material extrusion processes [71]. One interesting deviation from traditional composites is the introduction of filament strand boundaries in the matrix versus a continuous isotropic or laminate anisotropic matrix typically used in composites. The fiber-reinforced thermoplastic filament AM technique requires sufficient polymer bonding between the extruded thermoplastic filament strands to transfer the shear load to the fibers without causing fractures in the matrix between strands.

The doped filament AM process combine particles or short fibers with a polymer matrix such as ABS or PLA. Many different dopants are used in filaments to achieve specific properties such as conductivity, illumination, and textures [72–75]. Mechanical properties of parts manufactured by material extrusion have also been altered by the introduction of dopants including an iron doped nylon filament for direct tooling [76], iron and copper doped ABS for higher stiffness and improved thermal conductivity [77], and carbon nanotube doped ABS filaments for higher stiffness and up to a 39% increase in yield strength [78].

Embedding materials via thermal or ultrasonic techniques is one way to incorporate multiple materials in an AM manufacturing process. For instance, thermal embedding of copper wire into material extrusion thermoplastic structures can provide improved conductivity and mechanical strength [79]. The process incorporates metals into the FFF process creating three dimensional structural electronic components.

We previously developed the Fused Filament Fabrication-Stereolithography (F3SLA) process to combine the benefits of thermoplastic and photopolymer or other liquid resin materials in one AM process. A three axis gantry carries multiple extruders including a FFF thermoplastic extruder and a stepper-driven peristaltic liquid extruder to deliver photopolymers or other resins (two peristaltic liquid extruders are used in the case of two-part epoxies and resins). The first step in F3SLA manufacturing is the construction of a thermoplastic base shell. Two to three thermoplastic layers are used in the initial base to minimize leakage of liquid infill throughout later stages and one or two layer shells are constructed. As the build progresses layer by layer, liquid infill is pumped and deposited within the thermoplastic structure. The liquid extruder infills layers at a consistent two to three layers behind the thermoplastic sidewalls to ensure there is no overspill and that the FFF extruder tip does not contact liquid infill. Both photopolymers and quick set epoxies have been successfully tested using the F3SLA process [125,126].

4.2.6 Multifunctional and Tunable Materials

Multifunctional materials in AM were first presented through the integration of Vat Photopolymerization (VP) and Direct Write (DW) using conductive inks [80]. The idea of integrating VP and DW was aimed at creating structural components with embedded electronics, moving away from traditional structural shells with internal circuit boards and wire leads.

In summary, there are currently two economically priced and commercially available AM categories for engineers, hobbyists, and the maker community including Material Extrusion and Vat Photopolymerization. Material extrusion typically uses a three axis gantry to discretely deposit molten thermoplastics via a predefined toolpath to create three dimensional geometry. Vat Photopolymerization uses a “top up” or “bottom down” approach to construct three dimensional components layer by layer. Typically, in Vat Photopolymerization, either a laser traces each cross sectional layer (SLA) or a digital projector cures entire layers at once (DLP). Composites integrate

a matrix material (e.g.: thermoplastics, epoxies, photopolymers, etc.) with one or more phase materials (e.g.: fiberglass, carbon fiber, Kevlar, etc.) to achieve desired material properties not exhibited by the individual components. Composite AM approaches (e.g.: fiber-reinforced filaments, doped filaments, phase embedding, F3SLA, etc.) are uniquely suited for manufacturing composites due to the discrete deposition of feedstock material in AM. We present a hybrid composite AM methodology to provide the foundation for an AM toolset aimed at multi-material integration and tunable parameters.

4.3 Development of RF3SLA

In this section, we present the Reinforced Fused Filament Fabrication-Stereolithography (RF3SLA) process, a hybrid additive manufacturing method that provides a low cost option for fiber-reinforced composite AM. The RF3SLA process combines a thermoplastic extruder, liquid extruder, and fiber inlay extruder. This combination expands the material property design space and therefore results in more tunable material parameter options (e.g.: strength, fatigue life, stiffness, etc.) for students, engineers, hobbyists, and the maker community. In the development of RF3SLA we seek to expand the possibilities in low cost polymer additive manufacturing. In particular, we seek the ability to design and tune a part's mechanical properties through the integration of direct composite AM. The ability to design a part's mechanical properties through composite materials is a step towards multi-functional materials and reliable mechanical part integrity for low cost AM.

RF3SLA uses previous F3SLA development as a starting point to develop a true fiber reinforced composite AM process. We add reinforcement fibers deposited within the liquid infill layers. Using fibers in the liquid infill strengthens parts by transferring loads from the liquid infill matrix to the reinforcement fibers via shear stress. Fiber reinforcement can be deposited in any direction depending on mechanical apparatus limitations to support different load configurations.

This allows an operator to design the material properties of a structure itself, optimizing desired mechanical properties for specific applications.

Figure 4.1 demonstrates a generic RF3SLA extruder configuration. Three extrusion heads are included on a three axis gantry assembly including 1) a thermoplastic extruder, 2) a liquid resin extruder (one extruder in the case of photopolymers and one part epoxies or resins, two extruders in the case of two part epoxies or resins), and 3) a fiber extruder. The fiber extruder lays in fibers into a layer of liquid resin in the desired pattern, direction, and fiber length as specified by the designer or machine operator. The liquid layer is cured/photoset after the fibers have been inlaid. The next thermoplastic shell layer is then constructed, liquid resin is added, and the process is repeated until the desired part geometry is completed. Control of the three extruders is done through g-code that is generated either manually or in a custom slicer.

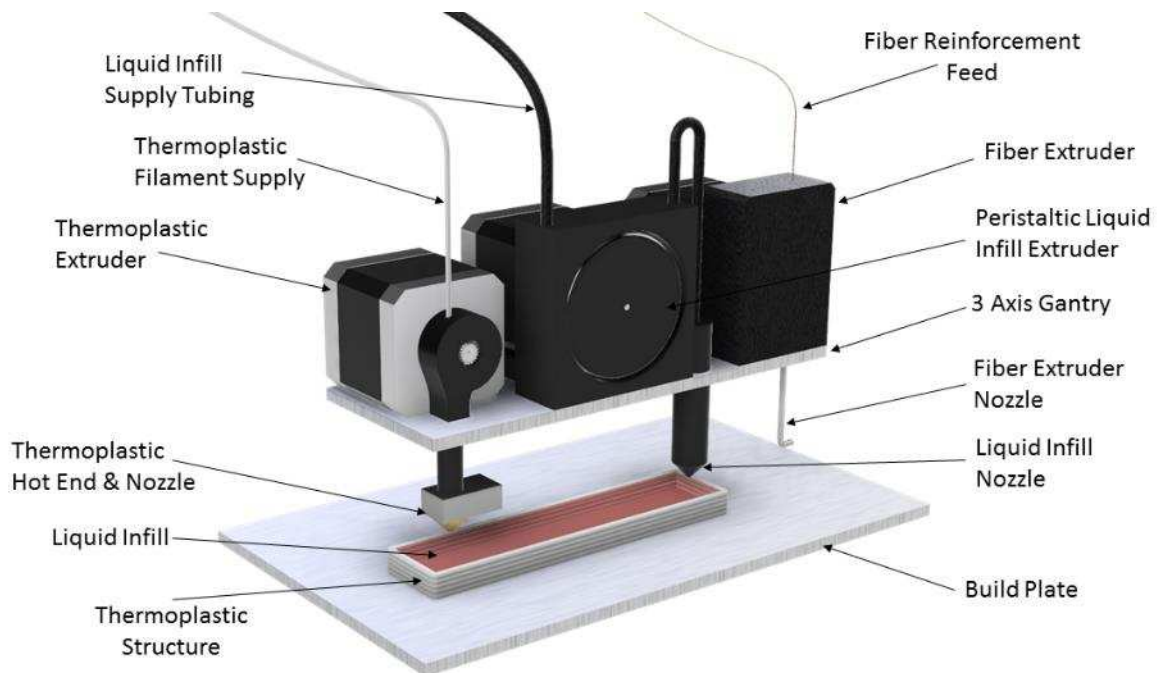


Figure 4.1: Possible RF3SLA Extruder Carriage Setup

Figure 4.2 shows a generic RF3SLA sample part. The thermoplastic outer structure layers are over emphasized by the change in grey tones. Multiple layers of continuous fiber

reinforcement can be seen within the liquid infill (red). Several fiber-inlay extruder designs allow for continuous global fiber reinforcement deposition, long fiber reinforcement deposition, or short fiber reinforcement deposition depending on the intended application.

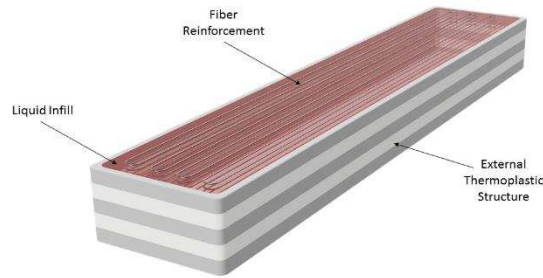


Figure 4.2: RF3SLA Sample

4.4 Material Testing of RF3SLA Parts

To validate RF3SLA as a viable AM method that can produce reliable parts with the flexibility of tunable parameters, we developed a material testing case study presented here. We selected two matrix materials (a photopolymer and an epoxy) to demonstrate that both can be successfully used. For each matrix material case we included four sets of eight test samples. The first set included only a thermoplastic shell and solid matrix core (no fiber reinforcement). The second case included two layers of evenly dispersed global fibers (140 mm) oriented along the axis of loading. The third case used the same total length (1.12 m) of long fibers (8 mm) near-randomly distributed along the axis of loading. The fourth case included the same total length (1.12 mm) of short fibers (2 mm) also distributed near-randomly within the matrix by mixing. We use soft Tex 120 Kevlar fiber for reinforcement because of the fiber's ease of use, high strength, and good fiber-matrix bonding strength. In addition to the eight RF3SLA cases, we included two control cases including a 100% concentrically infilled PLA sample manufactured by FFF and a 100% photopolymer case manufactured by DLP. The ten sample cases are summarized in Table 4.1.

Table 4.1: RF3SLA Case Study Overview

Sample Case	Shell Material	Infill Material	Reinforcement
Non-Reinforced Epoxy	Thermoplastic	Epoxy	
Global-Fiber Epoxy	Thermoplastic	Epoxy	Kevlar (140 mm)
Short-Fiber Epoxy	Thermoplastic	Epoxy	Kevlar (2 mm)
Long-Fiber Epoxy	Thermoplastic	Epoxy	Kevlar (8 mm)
Non-Reinforced Photopolymer	Thermoplastic	Photopolymer	
Global-Fiber Photopolymer	Thermoplastic	Photopolymer	Kevlar (140 mm)
Short-Fiber Photopolymer	Thermoplastic	Photopolymer	Kevlar (2 mm)
Long-Fiber Photopolymer	Thermoplastic	Photopolymer	Kevlar (8 mm)
100% Thermoplastic (FFF)	Thermoplastic	Thermoplastic	
100% Photopolymer (DLP)	Photopolymer	Photopolymer	

4.4.1 Coupon Production

We manufactured all coupons in-house with a two-step process, first printing the outer thermoplastic shell and second infilling the shell manually for RF3SLA samples. The shells were left uncapped by thermoplastic similar to the model in Figure 4.2 allowing the infill to be prepared off the build plate. We infilled the thermoplastic shell layer by layer to closely mimic how the samples are produced in the fully automated RF3SLA system described in Section 3. We chose to apply one liquid infill layer every two thermoplastic layers to speed the process up although the number of layers is tunable by the operator. The fiber reinforcement was deposited evenly at two different layers before the liquid layer cured to ensure maximum adhesion between the matrix infill and reinforcement. The completed photopolymer samples were put in a UV oven while the epoxy samples were set in a temperature-controlled environment as per the manufacturers' recommendations. For this case study we chose MakerJuice Labs G+ 3D Printing Ink v5 [109] as a photopolymer and Hatchbox Silver PLA 3D Printer Filament [114] as a thermoplastic due to both material's general purpose and widespread availability.

4.4.2 Material Testing

We performed tensile tests on the ten different cases to demonstrate the mechanical integrity and diverse mechanical property possibilities of RF3SLA parts through the pairing of multiple matrix and phase materials. We used 2D optical DIC strain measurement techniques to obtain an accurate strain measurement showing not only axial strain but also local strain on each coupon. Digital Image Correlation (DIC) is a full field measurement technique that compares digital images recorded throughout a material test to optically determine displacement and strain [81]. The DIC technique allowed us to visualize multi-material interactions across tensile loading to failure giving insight on the compatibility of various materials and effectiveness of load transfer throughout the AM composites by tracking changes in a black and white speck pattern [83]. Fiber optic lighting with polarization filters supplied sufficient illumination and minimized glare. Figure 4.3 shows a sample 2D DIC strain field overlain on a 100% infilled thermoplastic coupon produced through FFF. A complete set of strain field images can be found in [117].

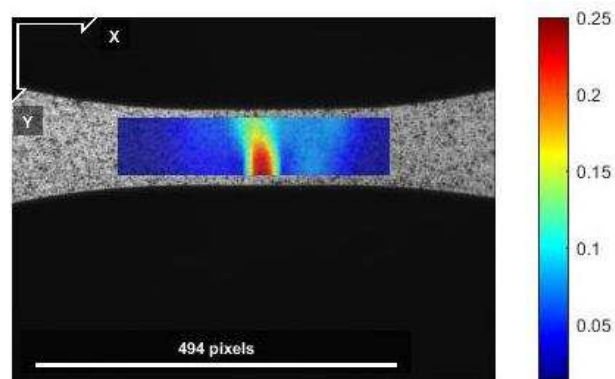


Figure 4.3: Sample 2D DIC Strain Field Overlay (100% Infill FFF)

Uniaxial tension tests were used for measuring material characteristics of both control cases and RF3SLA cases and provide quantitative comparisons (ultimate strength, specific strength, strain, etc.) for evaluating the mechanical integrity and material characteristic flexibility of each case. A Mark-10 [118] ESM1500 single-column force tester was used for all material

testing. A Mark-10 MR01-500 (500 lbf force limit) force sensors was used for all tension tests. Self-tightening wedge grips (Mark-10) were used for all tensile tests. All tests were conducted at a constant displacement rate of 5 mm/s. A Basler [119] acA645-100gm GigE camera with 659 x 494 pixel resolution and a frame rate of 10 hertz was used for optical strain measurement. This resolution gave us approximately 500 pixels for the testing region of the tensile samples. Additional image settings and external fiber optical lighting intensity (aperture, gain, etc.) were individually selected for each case to provide an optimal image quality depending on environmental lighting and subtle differences in speckle patterns between sample cases. Eight samples of each case were tested for both control and RF3SLA coupons. Figure 3.6 shows the geometry and dimensions for the tensile coupons in millimeters. The outer shell of all RF3SLA samples were solid infilled (rectilinear FFF) PLA.

4.5 Results

We present RF3SLA tensile test results in the following three subsections: photopolymer matrix results in Section 5.1, epoxy matrix results in Section 5.2, and a summary in Section 5.3 comparing photopolymer matrix results versus epoxy matrix results. Figures 4.4 and 4.5 report median stress-strain results while Table 4.2 reports various mean material properties for each case. Median plots were selected versus mean plots for reporting stress-strain curves to minimize the effects of skewness from outliers and therefore better represent the central tendency of the populations for the RF3SLA tensile test results.

4.5.1 Photopolymer RF3SLA

We present the results of the photopolymer RF3SLA tensile tests in a median stress-strain plot in Figure 4.4. The 100% thermoplastic sample case produced by FFF shows some necking before failure. The remainder of the samples including the 100% photopolymer sample case produced by DLP and the RF3SLA samples show brittle failures with no plastic deformation.

While the FFF and DLP samples have smooth stress-strain curves to failure, the RF3SLA samples cases all show minor failures along the path to some degree suggesting phase bonding failures, or micro-cracking before ultimate failure.

None of the photopolymer RF3SLA sample cases matched the 100% infilled thermoplastic FFF case in ultimate strength although there is improvement over the DLP photopolymer case. Both short-fiber reinforcement and long-fiber reinforcement in the photopolymer matrix had negative effects of the ultimate strength of a sample under tension as compared to non-reinforced samples. Global-fiber reinforcement in a photopolymer matrix resulted in an ultimate strength increase of 45% over non-reinforced RF3SLA photopolymer samples and 28% over DLP photopolymer samples.

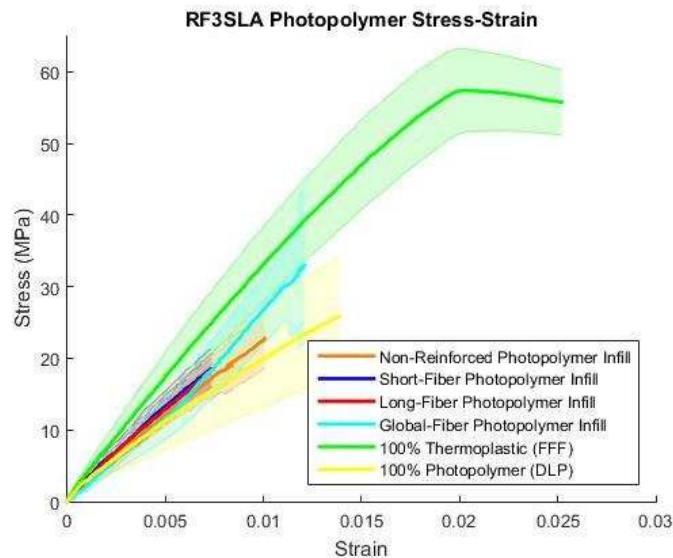


Figure 4.4: RF3SLA Stress-Strain Curves (Photopolymer)

4.5.2 Epoxy RF3SLA

We present the epoxy RF3SLA tensile test results in a median stress-strain plot shown in Figure 4.5. The epoxy matrix RF3SLA samples including global-fiber reinforced, long fiber reinforced, and short fiber reinforced all exhibited micro-cracking to a larger degree than their

corresponding photopolymer cases. Epoxy matrix samples additionally exhibited larger stress values at micro-cracking than photopolymers. Global fiber reinforced and long fiber reinforced epoxy RF3SLA test samples exhibited brittle failures while non-reinforced and short-fiber reinforced exhibited a plastic deformation region.

Globally-reinforced epoxy RF3SLA samples closely followed 100% thermoplastic samples manufactured by FFF in tensile performance. Non-reinforced and short-fiber reinforced epoxy RF3SLA samples failed closer to the DLP case than their corresponding photopolymer cases yet still failed at a lower ultimate stress. The long-fiber reinforced epoxy case performed better than both the long-fiber reinforced photopolymer case and the DLP case.

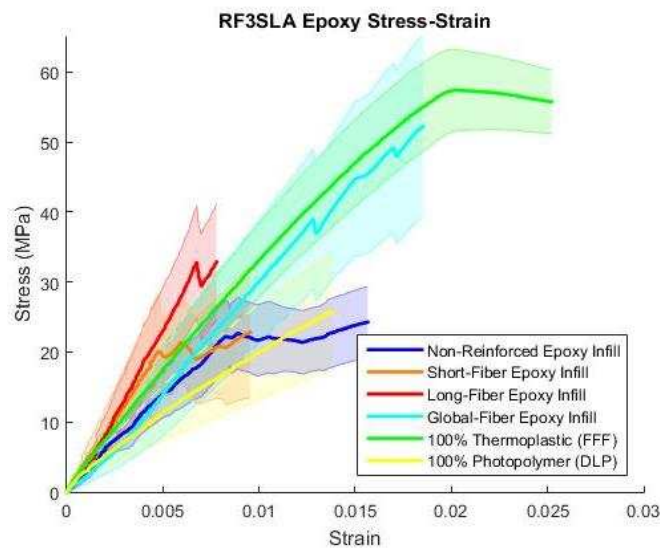


Figure 4.5: RF3SLA Stress-Strain Curves (Epoxy)

4.5.3 Result Summary

We present a summary of ultimate stress, ultimate strain, Young’s modulus, specific strength, and standard deviations for all samples as a means for comparison in Table 4.2. Table 4.2 was calculated from mean values versus median values presented in Figure 4.4 and Figure 4.5, resulting in higher reported values. Standard deviations for both ultimate stress and ultimate strain are reported as sample standard deviations. Young’s Modulus was calculated as the tangent

modulus for the linear elastic region of each sample case. This was achieved by manually selecting the linear region for each case and averaging the results across all eight samples. Note that the cases largely exhibit nonlinear responses and therefore the Young's modulus is only a valid measurement of material compliance within the linear elastic region.

Short-fiber reinforcement resulted in a 4% increase in ultimate strength and an 11% decrease in specific strength for an epoxy matrix. Short-fiber reinforcement resulted in a 16% decrease in ultimate strength and a 23% decrease in specific strength for a photopolymer matrix. Both epoxy matrix and photopolymer matrix RF3SLA samples exhibited a stiffer response with short-fiber reinforcement. A larger ultimate stress standard deviation was observed for short-fiber reinforced epoxy samples versus non-reinforced samples while a smaller ultimate stress standard deviation was observed for short-fiber reinforced photopolymers versus non-reinforced photopolymers.

Long-fiber reinforcement in an epoxy matrix resulted in a 41% increase in ultimate strength and a 23% increase in specific strength over non-reinforced epoxy. In a photopolymer matrix, long-fiber reinforcement resulted in an 11% decrease in ultimate strength and a 14% decrease in specific strength. Long-fiber reinforcement resulted in a stiffer response in both an epoxy matrix and a photopolymer matrix. Similarly to the effects of short-fiber reinforcement, long-fiber reinforcement exhibited a larger ultimate stress standard deviation in epoxy and smaller ultimate stress standard deviation in photopolymer with respect to the corresponding non-reinforced cases.

In an epoxy matrix, global-fiber reinforcement resulted in a 102% increase in ultimate strength and a 98% increase in specific strength. Global-fiber reinforcement resulted in a 33% increase in ultimate strength and a 48% increase in specific strength in a photopolymer matrix. Global-fiber reinforcement resulted in a stiffer response under tension as seen by short-fiber

reinforcement and long fiber reinforcement. Additionally, as seen by both short-fiber reinforcement and long-fiber reinforcement, global-fiber reinforcement exhibited a larger ultimate stress standard deviation in an epoxy matrix and a smaller ultimate stress standard deviation in a photopolymer matrix versus the corresponding non-reinforced cases.

The two highest performance materials were 100% thermoplastic and global-reinforced epoxy in terms of both ultimate stress and specific strength. Global-fiber reinforced photopolymer RF3SLA samples exhibited the third highest specific strength.

Table 4.2: RF3SLA Case Study Results Summary

Sample Case	Ultimate Stress (MPa)	Ultimate Stress Std. Dev.	Ultimate Strain	Ultimate Strain Std. Dev.	Young's Modulus (MPa)	Specific Strength (kPa/(kg/m³))
Non-Reinforced Epoxy	29.77	4.260	0.0141	0.0047	2833	25.68
Global-Fiber Epoxy	60.04	9.527	0.0187	0.0052	3039	50.88
Short-Fiber Epoxy	31.01	7.190	0.0093	0.0045	4130	22.84
Long-Fiber Epoxy	42.07	7.273	0.0107	0.0029	3799	31.48
Non-Reinforced Photopolymer	30.59	9.880	0.0141	0.0044	2362	29.59
Global-Fiber Photopolymer	40.56	8.637	0.0151	0.0034	2338	43.64
Short-Fiber Photopolymer	25.81	4.237	0.0113	0.0025	2581	22.89
Long-Fiber Photopolymer	27.24	6.107	0.0110	0.0033	2921	25.57
100% Thermoplastic (FFF)	60.28	1.710	0.0236	0.0016	3341	49.76
100% Photopolymer (DLP)	30.80	4.899	0.0213	0.0080	1978	23.04

4.6 Discussion

The following discussion provides our interpretations of the tensile tests presented in Section 5. We evaluate the selected epoxy and photopolymer as composite matrix materials and

the effectiveness of global-fiber reinforcement, long-fiber reinforcement, and short-fiber reinforcement. We additionally discuss RF3SLA's performance as compared to FFF and DLP.

Through the stress-strain trends presented in Figures 4.4 and 4.5, it is apparent that epoxy and photopolymer matrices act differently under tension. Photopolymer matrices for non-reinforced, short-fiber reinforced, long-fiber reinforced, and global-fiber reinforced cases all exhibit a linear stress-strain responses with minute micro-cracking and brittle failures. Epoxy matrices also exhibit linear stress-strain responses and a brittle failure for long-fiber reinforcement and global-fiber reinforcement although epoxy matrices perform differently for the non-reinforced and short-fiber reinforcement cases. Non-reinforced and short-fiber reinforced epoxies result in a linear elastic region followed by some degree of plastic deformation before failure. The larger stress values at micro-cracking for epoxy samples indicate that the epoxy used has a greater toughness than the photopolymer.

Short-fiber reinforcement is not an effective solution for improving mechanical performance, including ultimate strength, ultimate stress, and specific strength, in photopolymer or epoxy matrices. Short-fiber reinforcement exhibited an 11% decrease in specific strength for an epoxy matrix and 23% decrease in specific strength for a photopolymer matrix over non-reinforced matrices. While we do see a 4% increase in ultimate strength for short-fiber reinforced epoxies over non-reinforced epoxies, the decrease in specific strength and increase in ultimate strength standard deviation counter the ultimate strength improvement. Short-fiber reinforcement improves the ultimate stress standard deviation in a photopolymer matrix. We believe the decrease in standard deviation for short-fiber reinforced photopolymers may be due to the fiber providing localized support during photopolymer curing although more samples cases are needed for confirmation.

Long-fiber reinforcement provides conflicting results between epoxy and photopolymer matrix materials. In an epoxy matrix, long-fiber reinforcement results in a 23% specific strength increase and a 14% decrease in specific strength for a photopolymer matrix. Examining long-fiber failures, we see more fiber length protruding from the photopolymer matrix break than in the epoxy matrix case. The extra fiber indicates that we have matrix failure and therefore the photopolymer and Kevlar fiber are not good composite matrix-phase combination in the long fiber configuration. We see a similar trend in ultimate stress standard deviation for long-fiber reinforce as with short-fiber reinforcement.

Global-fiber reinforcement results in a decisive benefit for both epoxy and photopolymer matrices. In an epoxy matrix, global-fiber reinforcement exhibits a 98% increase in specific strength. In a photopolymer matrix, global fiber reinforcement exhibits a 48% increase in specific strength. Globally-reinforced epoxy and photopolymer matrix coupons experience different failure modes. Global reinforced epoxy matrix cores typically experience delamination and a shattering of matrix material at the center of the testing region. Global reinforced photopolymer matrix consistently fail at the outer regions of the reduced testing section. Photopolymer matrix failures often appear to stem from cracks formed from the self-tightening wedge grips of the load frame under large tension loads. Similarly to the long-fiber reinforcement case, we see less fiber protruding from the epoxy matrix than the photopolymer matrix indicating a better shear load transfer in the epoxy case.

Fiber reinforcement length in RF3SLA has different effects depending on matrix-phase pairing. From our investigation into matrix failures and fiber length performances in both epoxy and photopolymer matrix materials, it is apparent that matrix material selection and fiber pairing must be thoroughly studied before implementation. Regardless of matrix material, globally-

reinforced samples perform significantly better than non-reinforced, short-fiber reinforced, and long-fiber reinforced samples in both ultimate strength and specific strength. We see a significant increase in global-reinforced epoxy ultimate strain versus global-reinforced photopolymers indicating that the epoxy used bonded better to the Kevlar fiber.

To provide insight into effective use of RF3SLA, we split our RF3SLA material testing case study into different cases including epoxy matrix, photopolymer matrix, no-fiber reinforcement, short-fiber reinforcement, long-fiber reinforcement, and global-fiber reinforcement. Evaluating these cases on certain metrics such as ultimate strength, specific strength, stiffness, and repeatability we are able to identify above average performance for each matrix and phase material. The results are presented in Table 4.3. It should be noted that only one epoxy and photopolymer were tested in this case study and therefore these general recommendations may not be valid for every material in each case. Additional material testing and cataloging would allow for a larger database to be constructed for effective use of RF3SLA.

Table 4.3: RF3SLA Recommendations

Desired Parameter	RF3SLA Recommendation
Ultimate Strength	Epoxy Matrix, Global-Fiber Reinforcement
Specific Strength	Global-Fiber Reinforcement
Stiffer	Epoxy Matrix, Long-Fiber Reinforcement
More Compliant	Photopolymer Matrix, No Fiber Reinforcement
Repeatable	Short-Fiber Reinforcement

4.7 Conclusion and Future Work

In this paper, we demonstrate an improvement in mechanical integrity of components produced by RF3SLA over both FFF and DLP through an increase of up to 121% in specific strength over DLP and 2% over FFF using an epoxy matrix. While 2% does not seem like a significant improvement it should be noted that the 100% concentric infilled FFF control case is among the highest strength FFF sample and is rarely implemented in practice due to long

manufacturing times [120]. We also demonstrate the flexibility and tunability of material properties (e.g.: ultimate strength, elongation, specific strength, stiffness, etc.) in RF3SLA components through the use of two matrix materials and three fiber lengths. For an effective use of RF3SLA we suggest using an epoxy matrix and global-fiber reinforcement for high stress applications and a photopolymer matrix with no fiber reinforcement for applications requiring higher stiffness.

Further work on cataloging properties of additional materials will provide a database for RF3SLA mechanical property design of end use components. Repeatability must be improved by reducing standard deviations through process refinement to eliminate defects. Larger material testing case studies will also help verify property trends and provide a better baseline for tunable AM component design. CAD toolchain integration will then provide engineers, students, enthusiasts, and the maker community the necessary toolset to design high performance end-use AM components.

CHAPTER 5 AUTOMATION

In the previous two chapters, I introduced Fused Filament Fabrication-Stereolithography (F3SLA) and Reinforced F3SLA (RF3SLA) as hybrid additive manufacturing methods that provide low cost options for composite AM components with tunable parameters. This chapter focuses on the steps to integrate both F3SLA and RF3SLA into fully automated systems. I focus on automation of liquid infill, fiber-reinforcement deposition, and curing. From this point forward I solely look at RF3SLA but the reader is reminded that the F3SLA process is identical minus fiber-reinforcement deposition.

I first present a low level process diagram, displayed in Figure 5.1, showing how the RF3SLA process operates. RF3SLA manufactures composites through thermoplastic shells and liquid infill support. The process begins with a thermoplastic base of two to three layers to minimize liquid infill seepage before curing. The thermoplastic shell is then constructed layer by layer. As the shell is built, the liquid infill extruder deposits liquid infill inside the thermoplastic shell. The fiber deposition extruder then lays fiber-reinforcement in the predefined orientation and the liquid infill is cured or hardened depending on the infill type in use. The process is repeated until the geometry is finished as indicated by Figure 5.1. A thermoplastic cap then seals the part and the RF3SLA process is finished.

5.1 Steps Already Taken

The following sections outline the steps I have taken towards automation of the RF3SLA process and what future steps are anticipated. A 3D Systems CubeX Duo donor printer was obtained to be converted into the first ever RF3SLA printer [127]. Due to the proprietary nature of the CubeX Duo, I converted the printer to open source hardware and software for easy

modification. This was achieved through integration of a Megatronics V2.0 printer board, Pololu DRV8825 stepper drivers [128], and a standard desktop power supply.

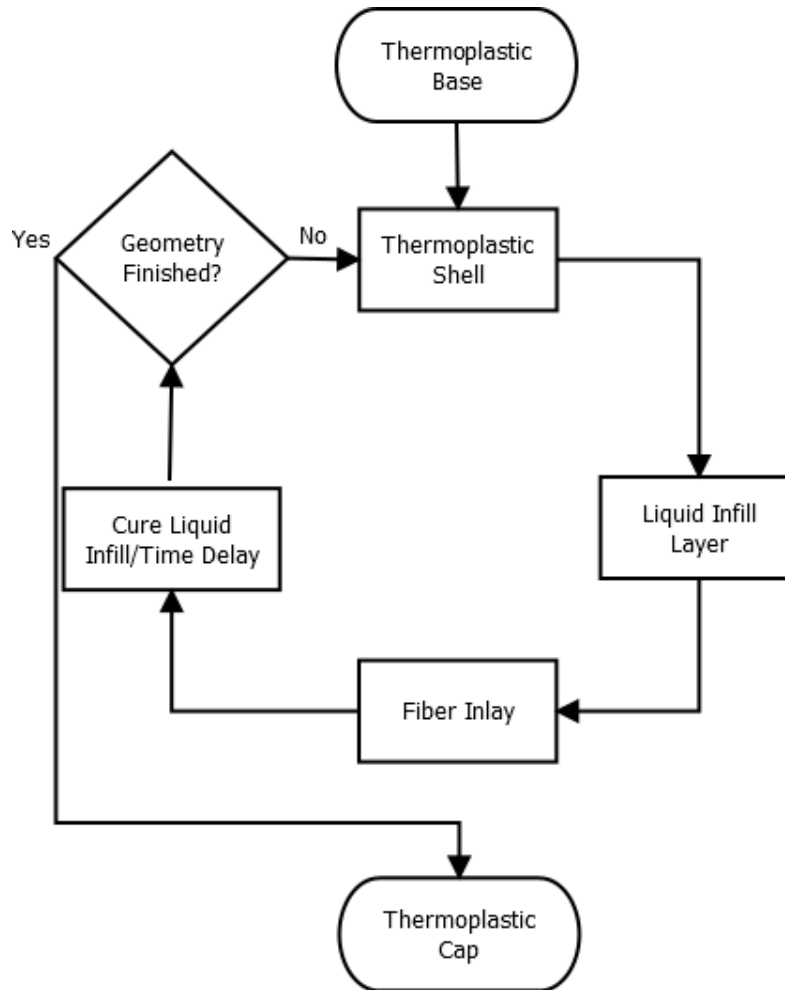


Figure 5.1: RF3SLA Process Diagram

After open source modifications to the printer were finished, I began RF3SLA modifications. This involved integrating several new subsystems into the printer including the liquid infill extruder system and the UV light rail. For the resin extruder subsystem, I designed and developed a stepper motor-driven peristaltic pump for precise deposition of liquid infill using identical controls as our thermoplastic extruders. The envisioned RF3SLA extruder head setup is shown in Figure 5.2. This setup shows three different extruders including a thermoplastic filament extruder, a liquid infill extruder, and a fiber deposition extruder.

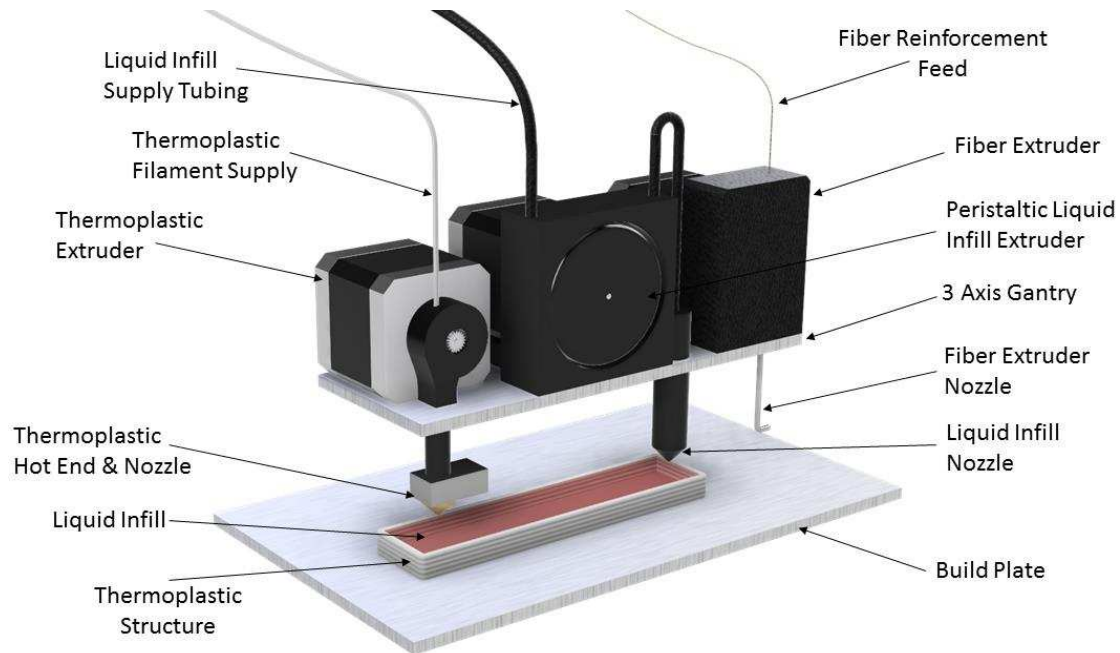


Figure 5.2: Envisioned RF3SLA Extruder Setup

Figure 5.3 shows the current extruder setup installed on the RF3SLA research printer. The stepper motor-driven peristaltic pump liquid infill extruder is shown (right) mounted next to the standard FFF thermoplastic extruder (left). A peristaltic pump was selected for liquid infill deposition to provide precise control over liquid flow, fast response time, identical control scheme to FFF extruders, easy cleanup, and easy transfer of liquid material supply lines. The fiber extruder is still undergoing preliminary testing and is not included in Figure 5.3.

Due to the high intensity ultra-violet (UV) light used for curing photopolymer infill. I designed, constructed and enclosed the RF3SLA printer in a blackout enclosure. Figure 5.4 shows the current RF3SLA setup including the blackout enclosure and control computer. Opaque photopolymer tubing and a shielded dump station were designed and integrated into the RF3SLA printer to protect uncured photopolymer in the supply tubing and nozzle residue from curing under UV bombardment. A camera has also been included to provide real-time monitoring of the printing procedure inside to the blackout enclosure.

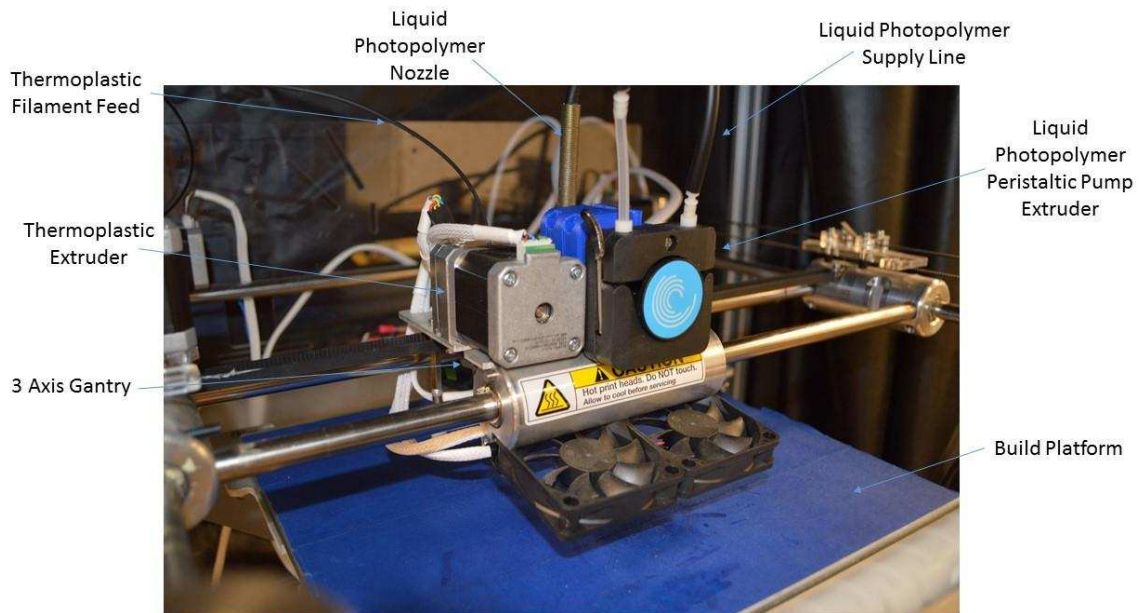


Figure 5.3: Current Extruder Setup

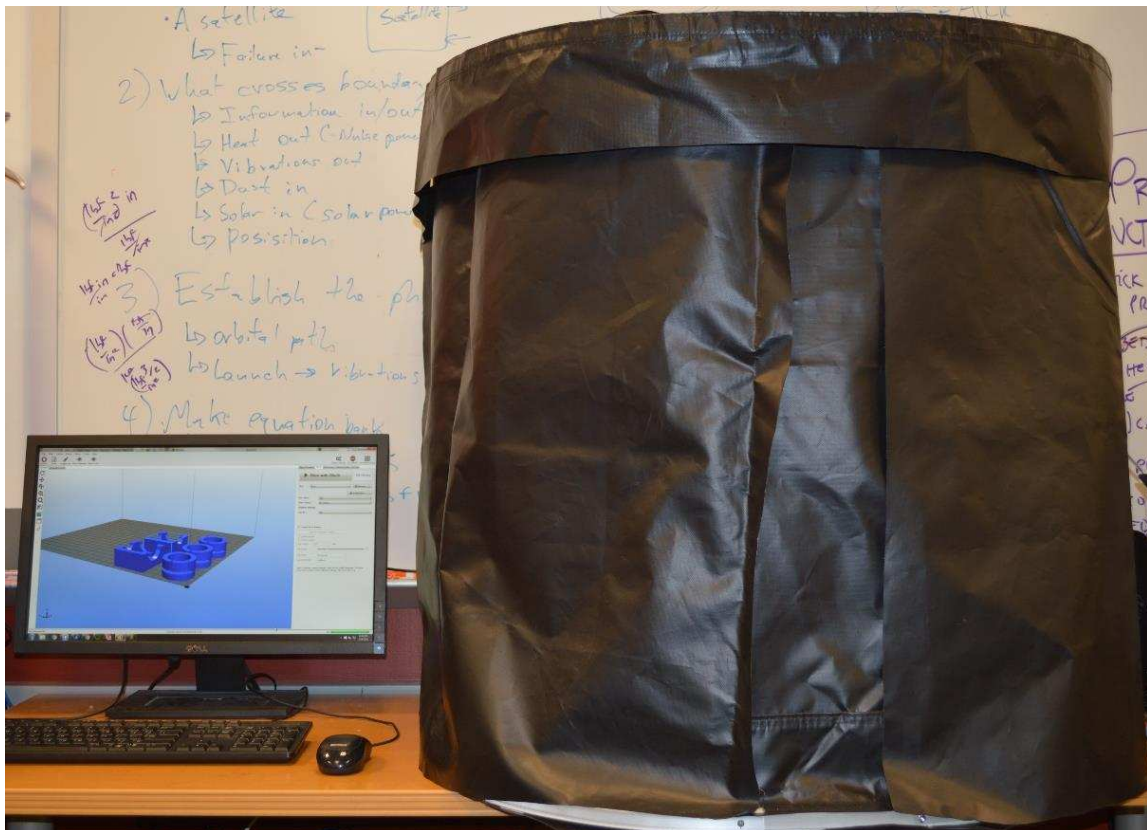


Figure 5.4: RF3SLA Printer in UV Safety Enclosure

5.2 Process Issues and Future Work

Several RF3SLA process issues that are still being worked towards mitigating include poor bonding of thermoplastic to cured photopolymer surfaces, curling of parts during photopolymer curing due to an exothermic reaction, pinning of fiber reinforcement during deposition in uncured liquid infill, and air pockets due to single layer photopolymer curling.

In addition to mitigating these issues, development of a RF3SLA slicer that better incorporates multiple material selection, various layer curing subroutines, and fiber deposition options including orientation, type (e.g.: short, long, or global), and density needs to be completed. The research presented in this thesis (especially Chapters 3 and 4) highlights the initial development, integration, and validation of F3SLA and RF3SLA although there are many additional steps that need to be addressed before full commercialization can be achieved. The major improvements needed include CAD toolset integration, further cataloging of RF3SLA materials, material interaction case studies to identify compatible materials, and development of commercial RF3SLA machines.

CHAPTER 6 CONCLUSIONS

A need for economical polymer AM components with mechanical integrity was identified in the introductory chapter of this thesis. Current low-cost AM machines (e.g.: material extrusion and vat photopolymerization) produce components that typically exhibit poor mechanical performance in contrast to bulk material properties. Several major factors have led to the premature adoption of low-end polymer AM for end-use components including: 1) the widespread availability of low cost AM machines including material extrusion and vat photopolymerization, 2) online businesses focused on economical quick turnaround manufacturing of AM parts, and 3) community funding of projects. This thesis proposes two economical composite AM processes that achieve improved mechanical integrity and material flexibility for low cost polymer AM.

6.1 Research Contributions

To meet the goal of providing an economical polymer AM option to produce components with mechanical integrity and material flexibility, I developed and validated two composite AM approaches including F3SLA and RF3SLA. The processes were evaluated on several metrics pertaining to part mechanical integrity including ultimate strength, specific strength, stiffness, and repeatability. This section reviews key results and conclusions drawn from the F3SLA case study, RF3SLA case study, and our automation efforts.

6.1.1 F3SLA Case Study Conclusions

F3SLA is a first step towards directly manufacturable low-cost composites through AM techniques. My research found F3SLA to be a viable option with many directions for future development. Initial test runs have successfully produced samples of several geometries. A set of suitable printing parameters were identified through process iterations and are ready to be incorporated in an automated process [117]. F3SLA brings new possibilities to the field of AM

by incorporating a wide range of materials in one process. While the framework for this method has been laid out, much more work is needed to bring this method to industry and the maker community. The first research phase presented here incorporated many parameter iterations making large data samples unfeasible. Future work will be needed to expand data sets and catalogue material mechanical properties to verify process robustness and provide a database for component design.

Although photopolymer infilled thermoplastic honeycomb samples were not successful in achieving a higher ultimate strength or specific strength, 100% infilled F3SLA samples did show potential. The 100% infilled photopolymer sample exhibited a 45% increase over 100% photopolymer samples produced by DLP and a 15% increase in ultimate strength over 50% infill density thermoplastics produced by FFF

6.1.2 RF3SLA Case Study Conclusions

In Chapter 4, I demonstrate an improvement in mechanical integrity of components produced by RF3SLA over both FFF and DLP through an increase of up to 121% in specific strength over DLP and 2% over FFF using an epoxy matrix. While 2% does not seem like a significant improvement it should be noted that the 100% concentric infilled FFF control case is among the highest strength FFF sample and is rarely implemented in practice due to long manufacturing times [120]. I also demonstrated the flexibility and tunability of material properties (e.g.: ultimate strength, elongation, specific strength, stiffness, etc.) in RF3SLA components through the use of two matrix materials and three fiber lengths. For an effective use of RF3SLA, I suggest using an epoxy matrix and global-fiber reinforcement for high stress applications and a photopolymer matrix with no fiber reinforcement for applications requiring higher stiffness.

6.2 Broader Impact

The process methodology and validation case studies presented in this thesis provide more design freedom and flexibility to students, engineers, enthusiasts, and the maker community. The underlying approach behind both F3SLA and RF3SLA enable both consumers and the technical committee to manufacture load-bearing components with mechanical integrity and material flexibility without sacrificing the ease of use, convenience, and economics of a low end polymer AM machine. Economical composite AM technologies will promote creativity, innovation, and technological growth by providing a manufacturing process aimed and low volume production runs and functional prototypes with a low barrier to entry.

6.3 Future Work

This section present future research directions spawned from the development and validation case studies of F3SLA and RF3SLA. Future work can be broken into three main categories including process tuning, material expansion, and implementation. Process tuning includes case studies on printing parameter variations such as layer heights, infill pattern, infill density, and extrusion temperature. Material expansion includes both a broadening of suitable materials for use in F3SLA and RF3SLA and material compatibility case studies aimed at exploring multiple material interactions between specific materials. Future work in implementation includes the design and testing of additional extruders to handle a wider range of materials, commercial machine development, and software development including an improved multi-material slicer and CAD integration.

Additional process tuning will improve mechanical properties (e.g.: ultimate strength, specific strength, stiffness, etc.) and manufacturing repeatability through the reduction of defects and better multi-material integration. Material testing case studies varying printing parameters for a series of materials will isolate printing properties beneficial to the F3SLA and RF3SLA

processes. Printing properties of specific interest spawned from the case studies presented in this thesis are infill type, infill density, layer height, and the combination of multi-material variations of these properties. For example, the variation of thermoplastic infill density and liquid polymer infill density.

Material expansion and cataloging will provide the basis for successful implementation of F3SLA and RF3SLA. A wider range of compatible materials will provide more flexibility in tuning mechanical parameters. An extensive material catalogue providing material properties for layer based components will provide students, engineers, enthusiasts, and the maker community with the data necessary to design high performance composite AM components. An expansion of compatible material types could also be explored such as ceramics to improve additional design parameters (e.g.: thermal management). Larger material testing case studies will also help verify property trends and provide a better baseline for tunable AM component design.

The implementation of F3SLA and RF3SLA can be broken into two main subsections including hardware development and software development. While the open source modifications necessary to perform F3SLA were presented in Chapter 3 and Chapter 5 of this thesis, commercial machines will provide a more user friendly F3SLA process integration. A fiber extruder design needs to be finalized and tested through additional RF3SLA case studies. Additional software development including CAD plugins and a slicer program specifically built for handling multi-material designs with fiber reinforcement need to be developed and implemented. A more in depth discussion regarding future work in hardware and software development can be found in Chapter 5.

6.4 Closing Thoughts

The economical polymer composite AM methodologies presented in this thesis provide a means to produce load-bearing, low production volume components and functional prototypes to

students, engineers, enthusiasts, and the maker community. To date, few low-end AM technologies provide design freedom and material flexibility. While new materials are under development, the composite AM processes presented, F3SLA and RF3SLA, provide an immediately available solution for low-end polymer AM components with mechanical integrity and material flexibility using commercially available materials. The hobbyist and maker community can immediately benefit from F3SLA and RF3SLA by implementing the processes on hobbyist AM machines. I expect these composite AM technologies and related processes to become available to engineers and AM service houses in the near future as commercial machines are developed using the methodologies presented.

REFERENCES CITED

- [1] M. Agarwala, Structural quality of parts processed by fused deposition, *Rapid Prototyp.* (1996). <http://www.emeraldinsight.com/doi/abs/10.1108/13552549610732034> (accessed February 16, 2016).
- [2] S.H. Huang, P. Liu, A. Mokasdar, L. Hou, Additive manufacturing and its societal impact: a literature review, *Int. J. Adv. Manuf. Technol.* 67 (2013) 1191–1203. doi:10.1007/s00170-012-4558-5.
- [3] M. Frohlich, R. Westbrook, Demand chain management in manufacturing and services: web-based integration, drivers and performance, *J. Oper. Manag.* (2002). <http://www.sciencedirect.com/science/article/pii/S0272696302000372> (accessed February 16, 2016).
- [4] P. MONEY, Crowd Funding: the Next Turnkey Financing Source for Entrepreneurs and Small Businesses, (n.d.). https://scholar.google.com/scholar?q=crowdfund+funding&btnG=&hl=en&as_sdt=0%2C6#2 (accessed February 16, 2016).
- [5] M. Ratto, R. Ree, Materializing information: 3D printing and social change, *First Monday.* (2012). <http://firstmonday.org/ojs/index.php/fm/article/viewArticle/3968> (accessed March 24, 2016).
- [6] R. Hague, I. Campbell, P. Dickens, Implications on design of rapid manufacturing, *Proc. Inst.* (2003). <http://pic.sagepub.com/content/217/1/25.short> (accessed March 24, 2016).
- [7] D. Bavishi, P. Shah, N. Patel, A. Shukla, V. Munde, Mass Customization of Products, *Citeseer.* (n.d.). <http://citeseerx.ist.psu.edu/viewdoc/download?doi=10.1.1.441.7302&rep=rep1&type=pdf> (accessed March 24, 2016).
- [8] T. Campbell, C. Williams, Could 3D printing change the world, ... *Addit. Manuf.* (2011). https://info.aiaa.org/SC/ETC/MS_SubCommittee/Alice_Chow_3D_Printing_Change_the_World_April_2012.pdf (accessed February 17, 2016).
- [9] A. International, Standard Terminology for Additive Manufacturing Technologies, *ASTM Int.* (2012) 10–12. doi:10.1520/F2792-12A.2.
- [10] J. Steuben, Design for Fused Filament Fabrication Additive Manufacturing, *ASME 2015* (2015). <http://proceedings.asmedigitalcollection.asme.org/proceeding.aspx?articleid=2483528> (accessed February 10, 2016).
- [11] A. Dolenc, I. Mäkelä, Slicing procedures for layered manufacturing techniques, *Comput. Des.* (1994). <http://www.sciencedirect.com/science/article/pii/0010448594900329> (accessed February 11, 2016).

- [12] P.M. Pandey, Slicing procedures in layered manufacturing: a review, *Rapid Prototyp. J.* ... (2003). <http://www.emeraldinsight.com/doi/pdf/10.1108/13552540310502185> (accessed February 11, 2016).
- [13] J. Hiller, H. Lipson, STL 2.0: a proposal for a universal multi-material additive manufacturing file format, *Proc. Solid Free. Fabr.* ... (2009). <http://citeseerx.ist.psu.edu/viewdoc/download?doi=10.1.1.475.5983&rep=rep1&type=pdf> (accessed February 10, 2016).
- [14] B.N. Turner, R. Strong, S.A. Gold, A review of melt extrusion additive manufacturing processes: I. Process design and modeling, *Rapid Prototyp. J.* (2014). <http://www.emeraldinsight.com/doi/abs/10.1108/RPJ-01-2013-0012> (accessed February 11, 2016).
- [15] I. Stratasys, Apparatus and method for creating three-dimensional objects, (1992). <http://www.google.com/patents/US5121329> (accessed March 20, 2016).
- [16] I. Gibson, D. Rosen, B. Stucker, *Additive manufacturing technologies*, 2010. <http://link.springer.com/content/pdf/10.1007/978-1-4939-2113-3.pdf> (accessed February 11, 2016).
- [17] F. Fischer, *Thermoplastics: The Best Choice for 3D Printing*, White Pap. Strat. Inc., Edn Prairie, MN. (2011). <http://www.tasman.com.au.spwd.net.nz/Portals/1/Public/SSYS-WP-Thermoplastics-05-11.pdf> (accessed February 12, 2016).
- [18] J. Giboz, T. Copponex, P. Mélé, Microinjection molding of thermoplastic polymers: a review, *J. Micromechanics* ... (2007). <http://iopscience.iop.org/article/10.1088/0960-1317/17/6/R02/meta> (accessed February 17, 2016).
- [19] P. Mallon, C. O'Brádaigh, R. Pipes, Polymeric diaphragm forming of complex-curvature thermoplastic composite parts, *Composites*. (1989). <http://www.sciencedirect.com/science/article/pii/0010436189906824> (accessed February 17, 2016).
- [20] S.-H. Ahn, M. Montero, D. Odell, S. Roundy, P.K. Wright, Anisotropic material properties of fused deposition modeling ABS, *Rapid Prototyp. J.* 8 (2002) 248–257. doi:10.1108/13552540210441166.
- [21] B.M. Tymrak, M. Kreiger, J.M. Pearce, Mechanical properties of components fabricated with open-source 3-D printers under realistic environmental conditions, *Mater. Des.* 58 (2014) 242–246. doi:10.1016/j.matdes.2014.02.038.
- [22] N. Mehat, S. Kamaruddin, Optimization of mechanical properties of recycled plastic products via optimal processing parameters using the Taguchi method, *J. Mater. Process. Technol.* (2011). <http://www.sciencedirect.com/science/article/pii/S0924013611001841> (accessed February 18, 2016).
- [23] C.W. Hull, Apparatus for production of three-dimensional objects by stereolithography,

- (1986). <http://www.google.com/patents/US4575330>.
- [24] F.P.W. Melchels, J. Feijen, D.W. Grijpma, A review on stereolithography and its applications in biomedical engineering., *Biomaterials*. 31 (2010) 6123. doi:10.1016/j.biomaterials.2010.04.050.
- [25] I. Campbell, I. Gibson, Additive manufacturing : rapid prototyping comes of age, (2012).
- [26] L.G. Zhang, J.P. Fisher, K. Leong, 3D Bioprinting and Nanotechnology in Tissue Engineering and Regenerative Medicine, Elsevier Science, 2015. <https://books.google.com/books?id=ud6cBAAQBAJ&pgis=1> (accessed April 1, 2016).
- [27] J. Stampfl, H. Fouad, S. Seidler, Fabrication and moulding of cellular materials by rapid prototyping, ... *Mater.* 21 (2004) 285–296. <http://www.inderscienceonline.com/doi/abs/10.1504/IJMPT.2004.004943> (accessed March 21, 2016).
- [28] R. Prototyp-, Curl Distortion Analysis During Photopolymerisation of, (2003) 586–595.
- [29] K. Altaf, I. a. Ashcroft, R. Hague, Modelling the effect of moisture on the depth sensing indentation response of a stereolithography polymer, *Comput. Mater. Sci.* 52 (2012) 112–117. doi:10.1016/j.commatsci.2011.01.051.
- [30] P. Jacobs, Rapid prototyping & manufacturing: fundamentals of stereolithography, 1992. <https://books.google.com/books?hl=en&lr=&id=y33AwAAQBAJ&oi=fnd&pg=PT5&dq=jacobs+fundamentals+of+stereolith&ots=gWiAB388Om&sig=qPKIXIGQ8tTxKR1W-h6ZPBurYII> (accessed February 22, 2016).
- [31] J. Beaman, J. Barlow, Solid freeform fabrication: a new direction in manufacturing, ... Publ. Norwell, MA. (1997). <http://link.springer.com/content/pdf/10.1007/978-1-4615-6327-3.pdf> (accessed February 22, 2016).
- [32] R. Harris, About Additive Manufacturing: Binder Jetting, Loughbrgh. Univ. (2016). <http://www.lboro.ac.uk/research/amrg/about/the7categoriesofadditivemanufacturing/binderjetting/>.
- [33] C. Groth, N. Kravitz, P. Jones, Three-dimensional printing technology, *J Clin* (2014). <http://www.kravitzorthodontics.com/assets/pdfs/3-Dimensional-Printing-Technology.pdf> (accessed February 11, 2016).
- [34] E. Sachs, J. Haggerty, Three-dimensional printing techniques, US Pat. 5,204,055. (1993). <https://www.google.com/patents/US5204055> (accessed February 24, 2016).
- [35] B. Utela, D. Storti, R. Anderson, M. Ganter, A review of process development steps for new material systems in three dimensional printing (3DP), *J. Manuf.* (2008). <http://www.sciencedirect.com/science/article/pii/S1526612509000206> (accessed February 24, 2016).

- [36] J. Bredt, T. Anderson, D. Russell, Three dimensional printing material system and method, US Pat. 6,610,429. (2003). <https://www.google.com/patents/US6610429> (accessed February 24, 2016).
- [37] R. Harris, About Additive Manufacturing: Material Jetting, Loughbrgh. Univ. (2016). <http://www.lboro.ac.uk/research/amrg/about/the7categoriesofadditivemanufacturing/materialjetting/>.
- [38] F. Gao, A. Sonin, Precise deposition of molten microdrops: the physics of digital microfabrication, ... R. Soc. London A (1994). <http://rspa.royalsocietypublishing.org/content/444/1922/533.short> (accessed February 24, 2016).
- [39] B. Tay, M. Edirisinghe, Investigation of some phenomena occurring during continuous ink-jet printing of ceramics, J. Mater. Res. (2001). http://journals.cambridge.org/abstract_S0884291400057812 (accessed February 24, 2016).
- [40] Q. Liu, M. Leu, M. Orme, High precision solder droplet printing technology: principle and applications, Adv. Packag. Mater. (2001). http://ieeexplore.ieee.org/xpls/abs_all.jsp?arnumber=916557 (accessed February 24, 2016).
- [41] R. Harris, About Additive Manufacturing: Powder Bed Fusion, Loughbrgh. Univ. (2016). <http://www.lboro.ac.uk/research/amrg/about/the7categoriesofadditivemanufacturing/powderbedfusion/>.
- [42] J. Beaman, C. Deckard, Selective laser sintering with assisted powder handling, US Pat. 4,938,816. (1990). <https://www.google.com/patents/US4938816> (accessed February 24, 2016).
- [43] L. Mullen, R. Stamp, Selective Laser Melting: A regular unit cell approach for the manufacture of porous, titanium, bone in-growth constructs, suitable for orthopedic applications, ... Res. Part B (2009). <http://onlinelibrary.wiley.com/doi/10.1002/jbm.b.31219/full> (accessed February 24, 2016).
- [44] Y. Hatta, T. Sakai, T. Shiraki, Melting titanium using electron beams; aircraft; corrosion resistance, US Pat. 6,918,942. (2005). <https://www.google.com/patents/US6918942> (accessed February 24, 2016).
- [45] S. Das, J. Beaman, Direct selective laser sintering of metals, US Pat. 6,676,892. (2004). <https://www.google.com/patents/US6676892> (accessed February 24, 2016).
- [46] R. Harris, About Additive Manufacturing: Directed Energy Deposition, Loughbrgh. Univ. (2016). <http://www.lboro.ac.uk/research/amrg/about/the7categoriesofadditivemanufacturing/directedenergydeposition/>.

- [47] T. Horn, O. Harrysson, Overview of current additive manufacturing technologies and selected applications, *Sci. Prog.* (2012).
<http://www.ingentaconnect.com/content/stl/sciprg/2012/00000095/00000003/art00003>
 (accessed February 10, 2016).
- [48] G. Lewis, R. Nemec, J. Milewski, D. Thoma, Directed light fabrication, (1994).
<http://www.osti.gov/scitech/biblio/10179475> (accessed February 24, 2016).
- [49] R. Harris, About Additive Manufacturing: Sheet Lamination, Loughbrgh. Univ. (2016).
<http://www.lboro.ac.uk/research/amrg/about/the7categoriesofadditivemanufacturing/sheetamination/>.
- [50] M. Feygin, S. Pak, Laminated object manufacturing apparatus and method, US Pat. 5,876,550. (1999). <https://www.google.com/patents/US5876550> (accessed February 24, 2016).
- [51] B. Mueller, D. Kochan, Laminated object manufacturing for rapid tooling and patternmaking in foundry industry, *Comput. Ind.* (1999).
<http://www.sciencedirect.com/science/article/pii/S0166361598001274> (accessed February 24, 2016).
- [52] D. White, D. Carmein, Ultrasonic object consolidation system and method, US Pat. 6,463,349. (2002). <https://www.google.com/patents/US6463349> (accessed February 24, 2016).
- [53] NDT Resource Center, Composite Structures, NDT Educ. Resour. Cent. (2014).
https://www.nde-ed.org/index_flash.htm (accessed January 1, 2016).
- [54] C. Bakis, L. Bank, V. Brown, Fiber-reinforced polymer composites for construction-state-of-the-art review, ... *Compos.* (2002).
[http://ascelibrary.org/doi/abs/10.1061/\(ASCE\)1090-0268\(2002\)6:2\(73\)](http://ascelibrary.org/doi/abs/10.1061/(ASCE)1090-0268(2002)6:2(73)) (accessed February 23, 2016).
- [55] R.E. Smallman, R.J. Bishop, *Metals and Materials: Science, Processes, Applications*, Elsevier, 2013. <https://books.google.com/books?id=MvwbQAAQBAJ&pgis=1>
 (accessed March 21, 2016).
- [56] M. Hyer, *Stress analysis of fiber-reinforced composite materials*, 2009.
https://books.google.com/books?hl=en&lr=&id=qgTVpw_uACoC&oi=fnd&pg=PR13&dq=Stress+Analysis+of+Fiber-reinforced+Composite+Materials&ots=o3gk6zPoaz&sig=xSIgAoJhq1xX8K67BZha6jOD3P0 (accessed February 24, 2016).
- [57] S. Fu, B. Lauke, Effects of fiber length and fiber orientation distributions on the tensile strength of short-fiber-reinforced polymers, *Compos. Sci. Technol.* (1996).
<http://www.sciencedirect.com/science/article/pii/S0266353896000723> (accessed February 10, 2016).

- [58] S. Advani, C.T. III, The use of tensors to describe and predict fiber orientation in short fiber composites, *J. Rheol.* (1987).
<http://scitation.aip.org/content/sor/journal/jor2/31/8/10.1122/1.549945> (accessed February 23, 2016).
- [59] J. McGrath, J. Wille, Determination of 3D fiber orientation distribution in thermoplastic injection molding, *Compos. Sci. Technol.* (1995).
<http://www.sciencedirect.com/science/article/pii/0266353895000127> (accessed February 23, 2016).
- [60] S.-Y. Fu, B. Lauke, The elastic modulus of misaligned short-fiber-reinforced polymers, *Compos. Sci. Technol.* 58 (1998) 389–400. doi:10.1016/S0266-3538(97)00129-2.
- [61] L. Monette, M.P. Anderson, G.S. Grest, The meaning of the critical length concept in composites: Study of matrix viscosity and strain rate on the average fiber fragmentation length in short-fiber polymer composites, *Polym. Compos.* 14 (1993) 101–115. doi:10.1002/pc.750140204.
- [62] T. Ohsawa, A. Nakayama, Temperature dependence of critical fiber length for glass fiber-reinforced thermosetting resins, *J. Appl.* (1978).
<http://onlinelibrary.wiley.com/doi/10.1002/app.1978.070221115/abstract> (accessed February 23, 2016).
- [63] P. Malnati, Reinforced Thermoplastics: LFRT/GMT Roundup, *Compos. Technol.* (2007).
<http://www.compositesworld.com/articles/reinforced-thermoplastics-lfirtgmt-roundup>.
- [64] T. Vu-Khanh, J. Denault, P. Habib, A. Low, The effects of injection molding on the mechanical behavior of long-fiber reinforced PBT/PET blends, *Compos. Sci. Technol.* 40 (1991) 423–435. doi:10.1016/0266-3538(91)90032-K.
- [65] T. Johnson, Continuous Fiber Thermoplastics, (2016).
<http://composite.about.com/od/Resins/a/Continuous-Fiber-Thermoplastics.htm>.
- [66] J. Wang, W. Chiu, Prediction of Matrix Failure in Fibre Reinforced Polymer Composites, *J. Eng.* (2013). <http://www.hindawi.com/journals/je/2013/973026/abs/> (accessed February 23, 2016).
- [67] B. Rosen, Tensile failure of fibrous composites, *AIAA J.* (1964).
<http://arc.aiaa.org/doi/abs/10.2514/3.2699> (accessed February 23, 2016).
- [68] P. Herrera-Franco, A. Valadez-Gonzalez, A study of the mechanical properties of short natural-fiber reinforced composites, *Compos. Part B Eng.* (2005).
<http://www.sciencedirect.com/science/article/pii/S1359836805000442> (accessed February 23, 2016).
- [69] L. Drzal, M. Madhukar, Fibre-matrix adhesion and its relationship to composite mechanical properties, *J. Mater. Sci.* (1993).
<http://link.springer.com/article/10.1007/BF01151234> (accessed February 11, 2016).

- [70] G. Mark, A. Gozdz, Apparatus for fiber reinforced additive manufacturing, US Pat. App. 14/333,947. (2014). <https://www.google.com/patents/US20140328963> (accessed February 24, 2016).
- [71] G. Mark, Methods for fiber reinforced additive manufacturing, US Pat. App. 14/297,437. (2014). <https://www.google.com/patents/US20140361460> (accessed February 24, 2016).
- [72] S. Leigh, R. Bradley, C. Purssell, A simple, low-cost conductive composite material for 3D printing of electronic sensors, PLoS One. (2012). <http://journals.plos.org/plosone/article?id=10.1371/journal.pone.0049365> (accessed February 24, 2016).
- [73] Y. Komatsu, K. Nakamura, Process for production of a carbon filament, US Pat. 4,816,289. (1989). <https://www.google.com/patents/US4816289> (accessed February 24, 2016).
- [74] J. Crawford, F. Traetz, Conductive filament, US Pat. 20,050,170,177. (2005). <http://www.freepatentsonline.com/y2005/0170177.html> (accessed February 24, 2016).
- [75] M. Feldman, B. Haynes, Electroluminescent filament, US Pat. 5,753,381. (1998). <https://www.google.com/patents/US5753381> (accessed February 24, 2016).
- [76] S. Masood, W. Song, Development of new metal/polymer materials for rapid tooling using fused deposition modelling, Mater. Des. (2004). <http://www.sciencedirect.com/science/article/pii/S0261306904000378> (accessed March 8, 2016).
- [77] M. Nikzad, S.H. Masood, I. Sbarski, Thermo-mechanical properties of a highly filled polymeric composites for Fused Deposition Modeling, Mater. Des. 32 (2011) 3448–3456. doi:10.1016/j.matdes.2011.01.056.
- [78] M. Shofner, Nanofiber-reinforced polymers prepared by fused deposition modeling, J. Appl. (2003). <http://onlinelibrary.wiley.com/doi/10.1002/app.12496/full> (accessed March 8, 2016).
- [79] D. Espalin, D. Muse, 3D Printing multifunctionality: structures with electronics, Int. J. (2014). <http://link.springer.com/article/10.1007/s00170-014-5717-7> (accessed March 8, 2016).
- [80] J. Palmer, Realizing 3-D interconnected direct write electronics within smart stereolithography structures, ASME 2005 (2005). <http://proceedings.asmedigitalcollection.asme.org/proceeding.aspx?articleid=1581387> (accessed March 7, 2016).
- [81] W. Peters, W. Ranson, Digital imaging techniques in experimental stress analysis, Opt. Eng. (1982). <http://opticalengineering.spiedigitallibrary.org/article.aspx?articleid=1222314> (accessed March 7, 2016).

- [82] P. Lava, S. Cooreman, D. Debruyne, Study of systematic errors in strain fields obtained via DIC using heterogeneous deformation generated by plastic FEA, *Opt. Lasers Eng.* (2010). <http://www.sciencedirect.com/science/article/pii/S0143816609002140> (accessed March 7, 2016).
- [83] M. Grediac, The use of full-field measurement methods in composite material characterization: interest and limitations, *Compos. Part A Appl. Sci. Manuf.* (2004). <http://www.sciencedirect.com/science/article/pii/S1359835X04000260> (accessed March 7, 2016).
- [84] K. V. Wong, A. Hernandez, A Review of Additive Manufacturing, *ISRN Mech. Eng.* 2012 (2012) 1–10. doi:10.5402/2012/208760.
- [85] C. Williams, Towards the Design of a layer-based additive manufacturing process for the realization of metal parts of designed mesostructure, *16th Solid* (2005). http://westinghouse.gtmi.gatech.edu/Members/cwilliams/papers/CBW_SFF05_Draft.pdf (accessed February 11, 2016).
- [86] F. Sonmez, H. Hahn, Thermomechanical analysis of the laminated object manufacturing (LOM) process, *Rapid Prototyp. J.* (1998). <http://www.emeraldinsight.com/doi/abs/10.1108/13552549810197541> (accessed February 11, 2016).
- [87] K.P. Karunakaran, S. Suryakumar, V. Pushpa, S. Akula, Low cost integration of additive and subtractive processes for hybrid layered manufacturing, *Robot. Comput. Integr. Manuf.* 26 (2010) 490–499. doi:10.1016/j.rcim.2010.03.008.
- [88] S. Akula, K.P. Karunakaran, Hybrid adaptive layer manufacturing: An Intelligent art of direct metal rapid tooling process, *Robot. Comput. Integr. Manuf.* 22 (2006) 113–123. doi:10.1016/j.rcim.2005.02.006.
- [89] R. Ma, J. Belter, A. Dollar, Hybrid deposition manufacturing: Design strategies for multimaterial mechanisms via Three-Dimensional printing and material deposition, *J.* (2015). <http://thermalscienceapplication.asmedigitalcollection.asme.org/article.aspx?articleid=2085506> (accessed February 12, 2016).
- [90] B. Wendel, D. Rietzel, Additive processing of polymers, *Macromol.* (2008). <http://onlinelibrary.wiley.com/doi/10.1002/mame.200800121/full> (accessed February 11, 2016).
- [91] H. Brooks, Variable fused deposition modelling-concept design and tool path generation, (2011). <http://clock.uclan.ac.uk/3864/> (accessed February 11, 2016).
- [92] ASTM Norma, Standard Test Method for Tensile Properties of Plastics, *Annu. B. ASTM Stand.* (2004) 1–15. doi:10.1520/D0638-14.1.
- [93] P. Lin, K. Willis, INTELLIGENT 3D PRINTING THROUGH OPTIMIZATION OF 3D

- PRINT PARAMETERS, US Pat. (2015).
<http://www.freepatentsonline.com/y2015/0331402.html> (accessed February 11, 2016).
- [94] S. Suryakumar, K.P. Karunakaran, A. Bernard, U. Chandrasekhar, N. Raghavender, D. Sharma, Weld bead modeling and process optimization in Hybrid Layered Manufacturing, *Comput. Des.* 43 (2011) 331–344. doi:10.1016/j.cad.2011.01.006.
- [95] P. Cignoni, M. Callieri, Meshlab: an open-source mesh processing tool., *Eurographics Ital.* (2008).
https://www.researchgate.net/profile/Paolo_Cignoni/publication/221210477_MeshLab_an_Open-Source_Mesh_Processing_Tool/links/54e45d130cf2dbf60695de7d.pdf (accessed February 11, 2016).
- [96] J. Stampfl, S. Baudis, C. Heller, Photopolymers with tunable mechanical properties processed by laser-based high-resolution stereolithography, *J.* (2008).
<http://iopscience.iop.org/article/10.1088/0960-1317/18/12/125014/meta> (accessed February 11, 2016).
- [97] A. Capel, S. Edmondson, S. Christie, Design and additive manufacture for flow chemistry, *Lab Chip.* (2013). <http://pubs.rsc.org/en/content/articlehtml/2013/lc/c3lc50844g> (accessed February 12, 2016).
- [98] Z. Quan, A. Wu, M. Keefe, X. Qin, J. Yu, J. Suhr, et al., Additive manufacturing of multi-directional preforms for composites: opportunities and challenges, *Mater. Today.* 18 (2015) 503–512. doi:10.1016/j.mattod.2015.05.001.
- [99] J. Holbery, D. Houston, Natural-fiber-reinforced polymer composites in automotive applications, *Jom.* (2006). <http://link.springer.com/article/10.1007/s11837-006-0234-2> (accessed February 11, 2016).
- [100] L. Hollaway, *Handbook of polymer composites for engineers*, 1994.
https://books.google.com/books?hl=en&lr=&id=drGjAgAAQBAJ&oi=fnd&pg=PP1&dq=composite+manufacturing+RIM&ots=2qDyoCwhih&sig=iVDsD5zR5DJDsCKnJHibjxSdm_Q (accessed February 11, 2016).
- [101] K. Oksman, High quality flax fibre composites manufactured by the resin transfer moulding process, *J. Reinf. Plast. Compos.* (2001).
<http://jrp.sagepub.com/content/20/7/621.short> (accessed February 11, 2016).
- [102] R. Sadeghian, S. Gangireddy, Manufacturing carbon nanofibers toughened polyester/glass fiber composites using vacuum assisted resin transfer molding for enhancing the mode-I, ... *Manuf.* (2006). <http://www.sciencedirect.com/science/article/pii/S1359835X05003775> (accessed February 11, 2016).
- [103] J. Acheson, P. Simacek, S. Advani, The implications of fiber compaction and saturation on fully coupled VARTM simulation, ... *Appl. Sci. Manuf.* (2004).
<http://www.sciencedirect.com/science/article/pii/S1359835X03003269> (accessed February 11, 2016).

- [104] R. Gibson, Principles of composite material mechanics, 2011. https://books.google.com/books?hl=en&lr=&id=vxg9Z4aJ36MC&oi=fnd&pg=PP1&dq=composite+material+testing&ots=n_sdE-L47s&sig=giLAeZBQa8GyV7g1dIRNtDBj4Zs (accessed February 11, 2016).
- [105] R. Selzer, K. Friedrich, Mechanical properties and failure behaviour of carbon fibre-reinforced polymer composites under the influence of moisture, *Compos. Part A Appl. Sci.* (1997). <http://www.sciencedirect.com/science/article/pii/S1359835X96001546> (accessed February 11, 2016).
- [106] W. Callister, D. Rethwisch, Materials science and engineering: an introduction, 2007. [https://smccd-public.sharepoint.com/CanCurriculumCommittee/Articulation/SampleCourseOutlines/Engineering/ENGR 260 - Cuyamaca.pdf](https://smccd-public.sharepoint.com/CanCurriculumCommittee/Articulation/SampleCourseOutlines/Engineering/ENGR260-Cuyamaca.pdf) (accessed February 11, 2016).
- [107] MarkForged, No Title, (n.d.). <https://markforged.com/>.
- [108] O. Ivanova, C. Williams, T. Campbell, Additive manufacturing (AM) and nanotechnology: promises and challenges, *Rapid Prototyp. J.* 19 (2013) 353–364. doi:10.1108/RPJ-12-2011-0127.
- [109] MakerJuice Labs, MakerJuice Labs LLC. (n.d.). www.makerjuice.com.
- [110] MakerBot, MakerBot Ind. LLC. (n.d.). www.makerbot.com.
- [111] MakerGear, MakerGear LLC. (n.d.). www.makergear.com.
- [112] ASTM F2971 - 13 Standard Practice for Reporting Data for Test Specimens Prepared by Additive Manufacturing, (2013). <http://www.astm.org/Standards/F2971.htm> (accessed February 11, 2016).
- [113] ASTM D638-14, Standard Test Method for Tensile Properties of Plastics, ASTM Int. West Conshohocken, PA. (2014). www.astm.org.
- [114] HATCHBOX, (2016). <http://www.hatchbox3d.com>.
- [115] J. Blaber, Ncorr v1.2, Open Source. (2016). www.ncorr.com.
- [116] J. Blaber, B. Adair, A. Antoniou, Ncorr: open-source 2D digital image correlation matlab software, *Exp. Mech.* (2015). <http://link.springer.com/article/10.1007/s11340-015-0009-1> (accessed February 12, 2016).
- [117] R. Hemphill, Development and Validation of a Hybrid Additive Manufacturing Method, Colorado School of Mines, 2016.
- [118] MARK-10, Force & Torque Measurement Engineered Better, (n.d.). <http://www.mark-10.com/>.
- [119] Basler, Basler the power of sight, (n.d.). <http://www.baslerweb.com/en>.

- [120] 3D Matter, What is the influence of infill %, layer height and infill pattern on my 3D prints?, (2015). <http://www.my3dmatter.com/influence-infill-layer-height-pattern/>.
- [121] Kudo3D, Recommended Printing Parameters: Exposure Time, Lifting Height, & Lifting Speed, Kudo3D Inc. (2016). <http://www.kudo3d.com/recommended-printing-parameters-exposure-time-lifting-height-lifting-speed/>.
- [122] B. Berman, 3-D printing: The new industrial revolution, *Bus. Horiz.* (2012). <http://www.sciencedirect.com/science/article/pii/S0007681311001790> (accessed February 16, 2016).
- [123] C. Christensen, The innovator's dilemma: when new technologies cause great firms to fail, 2013. <https://books.google.com/books?hl=en&lr=&id=3JnBAgAAQBAJ&oi=fnd&pg=PR4&dq=The+innovator%E2%80%99s+dilemma:+when+new+technologies+cause+great+firms+to+fail&ots=G3z25RfqYV&sig=HvJpwB1jS6lKD5jd4Py73lz66rg> (accessed February 16, 2016).
- [124] E. MacDonald, R. Salas, D. Espalin, 3D printing for the rapid prototyping of structural electronics, *Access*, (2014). http://ieeexplore.ieee.org/xpls/abs_all.jsp?arnumber=6766751 (accessed March 24, 2016).
- [125] R. Hemphill, D. Van Bossuyt, Manufacturing Composites Utilizing a Hybrid Material Extrusion-Photopolymerization Approach, *Prep. Rapid Prototyp. J.* (n.d.).
- [126] R. Hemphill, K. Young, M. Harris, A. Short, D. Van Bossuyt, Hybrid Additive Manufacturing Method, Provisional Patent Application No. 62/212,401, 2015.
- [127] 3DSystems, 3D Syst. Inc. (2015). www.3dsystems.com.
- [128] Pololu, Pololu Corp. (2016). <https://www.pololu.com>.

APPENDIX A

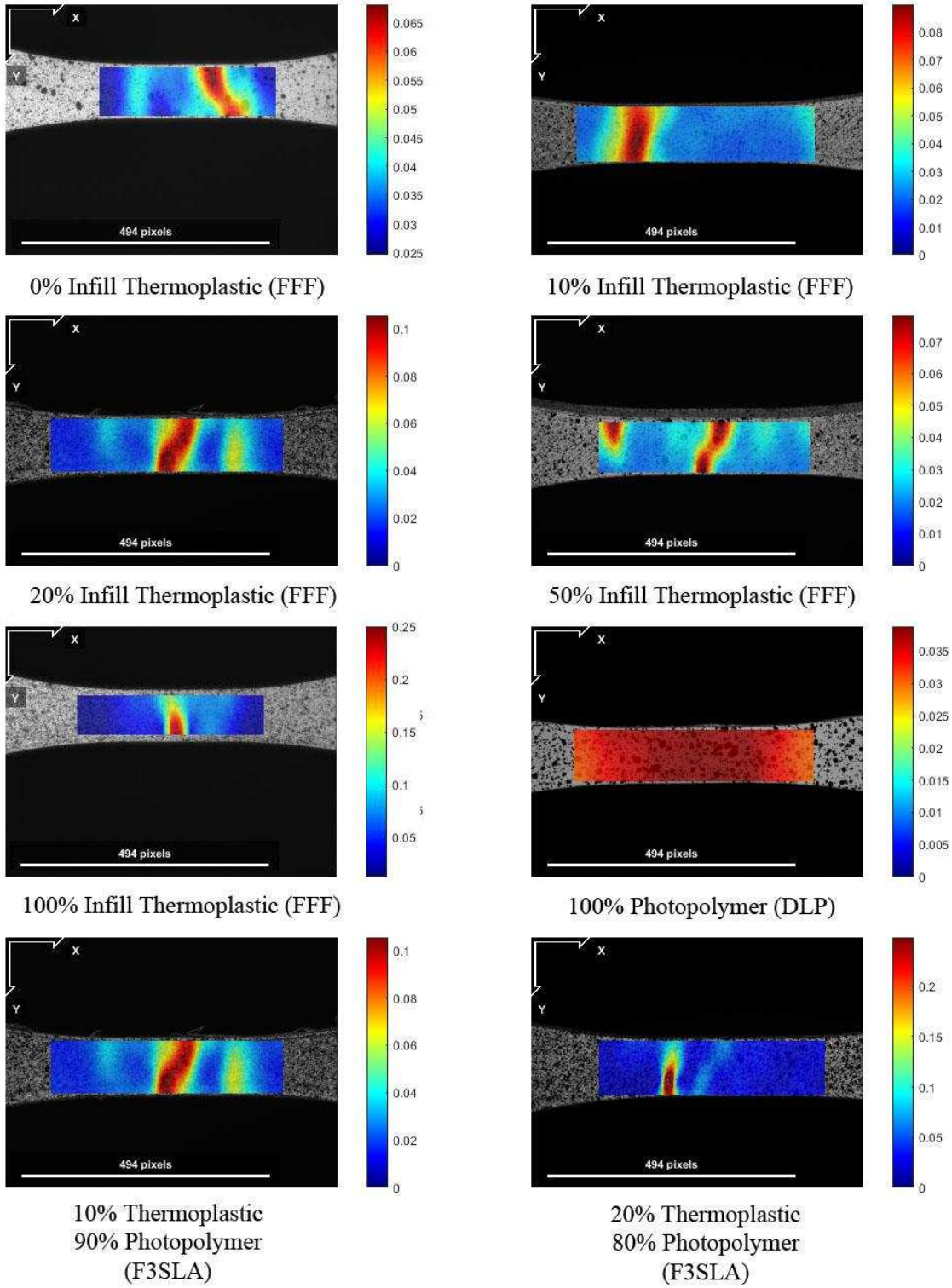
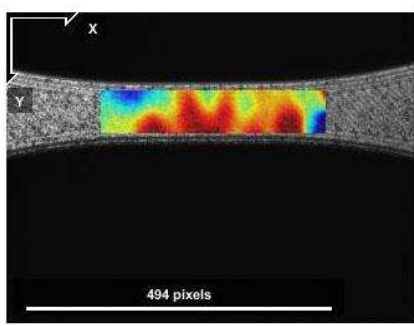
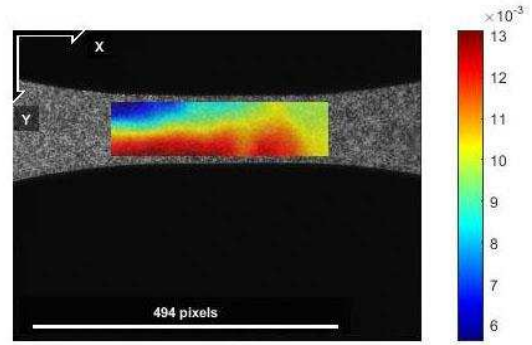


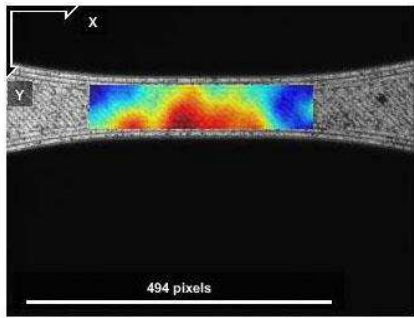
Figure A-1: Full Sample of F3SLA Ultimate Strain Fields



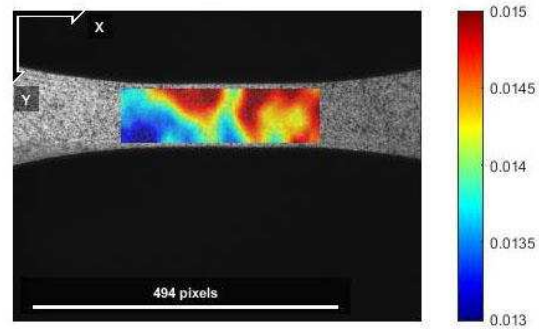
Non-Reinforced Photopolymer (RF3SLA)



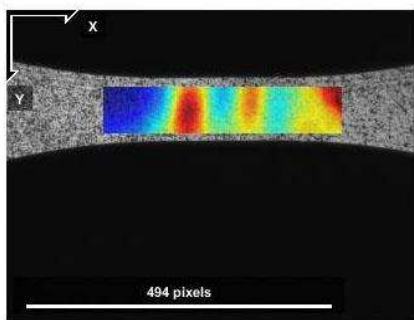
Short-Reinforced Photopolymer (RF3SLA)



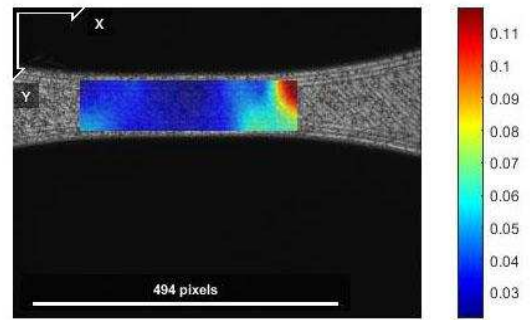
Long-Reinforced Photopolymer (RF3SLA)



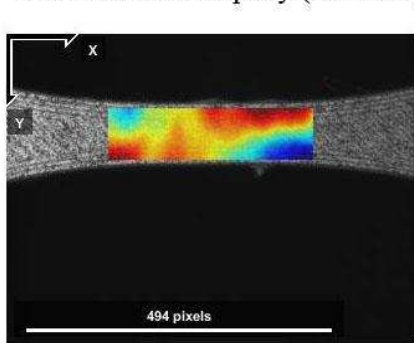
Global-Reinforced Photopolymer (RF3SLA)



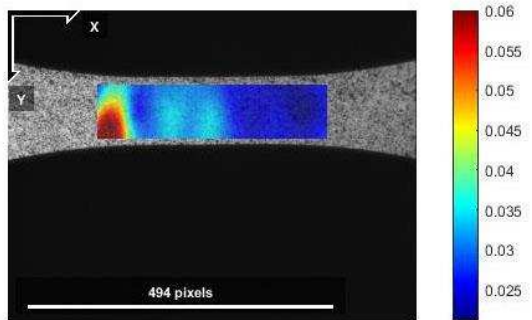
Non-Reinforced Epoxy (RF3SLA)



Short-Reinforced Epoxy (RF3SLA)



Long-Reinforced Epoxy (RF3SLA)



Global-Reinforced Epoxy (RF3SLA)

Figure A-2: Full Sample of RF3SLA Ultimate Strain Fields

APPENDIX B

Table B-1: F3SLA Coupon Printing Parameters

F3SLA Coupon Printing Parameters	
Host Software	Repetier-Host v1.6.0
Slicer Software	Slic3r
Printer	MakerGear M2 (24 v)
Nozzle Diameter	0.4 mm
Filament Diameter	1.75 mm
Layer Height	0.3 mm
Vertical Shells	3
Horizontal Shells	3 Bottom, 3 Top
Infill Type	Honeycomb
Top/Bottom Fill Pattern	Rectilinear
Extruder Temperature	230 °C
Bed Temperature	100 °C
Standard Print Speed	80 mm/s
Infill Print Speed	80 mm/s
Solid Infill Print Speed	50 mm/s
Top Layer Print Speed	30 mm/s
First Layer Print Speed	40 mm/s
Travel Speed	90 mm/s

Table B-2: RF3SLA Coupon Printing Parameters

RF3SLA Coupon Printing Parameters	
Host Software	Repetier-Host v1.6.0
Slicer Software	Slic3r
Printer	MakerGear M2 (24 v)
Nozzle Diameter	0.4 mm
Filament Diameter	1.75 mm
Layer Height	0.3 mm
Vertical Shells	3
Horizontal Shells	3 Bottom, 0 Top
Infill Type	Concentric
Top/Bottom Fill Pattern	Rectilinear
Extruder Temperature	230 °C
Bed Temperature	100 °C
Standard Print Speed	80 mm/s
Infill Print Speed	N/A
Solid Infill Print Speed	50 mm/s
First Layer Print Speed	40 mm/s
Travel Speed	90 mm/s